Three-dimensional lattice multiflavor scalar chromodynamics: Interplay between global and gauge symmetries

Claudio Bonati,[1] Andrea Pelissetto,[2] and Ettore Vicari[1]

[1]*Dipartimento di Fisica dell'Università di Pisa and INFN, Largo Pontecorvo 3, I-56127 Pisa, Italy*
[2]*Dipartimento di Fisica dell'Università di Roma Sapienza and INFN, Sezione di Roma I, I-00185 Roma, Italy*

(Received 8 January 2020; accepted 21 January 2020; published 10 February 2020)

We study the nature of the finite-temperature transition of the three-dimensional scalar chromodynamics with N_f flavors. These models are constructed by considering maximally O(M)-symmetric multicomponent scalar models, whose symmetry is partially gauged to obtain SU(N_c) gauge theories, with a residual nonabelian global symmetry given by $U(N_f)$ for $N_c \geq 3$ and Sp(N_f) for $N_c = 2$, so that $M = 2N_cN_f$. For $N_f = 2$ and for all values of N_c we investigated, $N_c = 2$, 3, 4, these systems undergo a continuous finite-temperature transition, which belongs to a universality class related to the global symmetry group of the model. For $N_c = 2$, since $\mathrm{Sp}(2)/\mathbb{Z}_2 = \mathrm{SO}(5)$, it belongs to the O(5) vector universality class. For $N_c \geq 3$, since $\mathrm{SU}(2)/\mathbb{Z}_2 = \mathrm{SO}(3)$, it belongs to the O(3) vector universality class. For $N_f \geq 3$, the numerical results show evidence of first-order transitions for any N_c. These results are in agreement with the predictions obtained by using the effective Landau-Ginzburg-Wilson approach in terms of a gauge-invariant order parameter. Our results indicate that the non-Abelian gauge degrees of freedom are irrelevant at the transition. These conclusions are supported by an analysis of gauge-field dependent correlation functions, that are always short ranged, even at the transition.

DOI: 10.1103/PhysRevD.101.034505

I. INTRODUCTION

The importance of symmetries in modern physics can be hardly overestimated. Global symmetries and the way in which they are realized are commonly used to identify and describe different phases of matter [1]. Local gauge symmetries play a fundamental role both in particle physics, where they lie at the heart of the Standard Model [2], and in condensed-matter physics, where their applications span from superconductivity [3] to topological order and quantum phase transitions [4].

Several systems of physical interest display both global and local gauge symmetries, and a fundamental problem is to understand which of these symmetries play a role in determining the universal behavior of the system close to a continuous phase transition. The traditional Landau-Ginzburg-Wilson (LGW) approach to critical phenomena relies on statistical field theory [5–9]. In this scheme, critical properties depend only on the global symmetry breaking pattern and on some "kinematic" parameters, like the space dimensionality and the number of field components. For transitions to/from topologically ordered states, this time-honored scheme has to be modified, due to the peculiar nonlocal character of topological order [10,11]. However, when a continuous phase transition emerges due to the breaking of a global symmetry in a gauge theory, it is by no means obvious which is the role played by the gauge degrees of freedom (d.o.f.): do they affect the critical behavior or not?

The study of the chiral phase transition in massless quantum chromodynamics (QCD) was likely the first occasion in which this problem could have been raised. Massless QCD is indeed invariant under local SU(3) color transformations and under global $\mathrm{SU}_L(N_f) \times \mathrm{SU}_R(N_f)$ flavor transformations, with the chiral transition being associated with the symmetry breaking pattern $\mathrm{SU}_L(N_f) \times \mathrm{SU}_R(N_f) \to \mathrm{SU}_V(N_f)$ [2]. However, starting from the seminal work of Pisarski and Wilczek [12] (see Refs. [13,14] for some refinements), it was always implicitly assumed that gauge d.o.f. are irrelevant at the chiral transition, whose properties were predicted by using a gauge-invariant order parameter and the LGW approach. Numerical lattice results later supported these predictions, although with limited numerical precision because of the computational burden of simulating dynamical fermions. Moreover, in recent times, possible hints of discrepancies have appeared (see Refs. [15,16] for recent reviews).

The dependence of the critical behavior on the gauge d.o.f. can be numerically investigated more accurately in scalar models. The three-dimensional (3D) Abelian case has recently attracted much attention, both from the theoretical and from the numerical point of view [10,11,17–25]. In particular, some works [22–25] reported some numerical evidence that the LGW approach, based on a gauge-invariant

order parameter, may not describe the emerging critical behavior.

Notwithstanding their applications to high-energy physics (most notably to the QCD chiral phase transition but also to possible extensions of the standard model) and their growing importance in condensed-matter physics [4,11,26,27], 3D multiflavor scalar non-Abelian gauge theories have been much less studied so far. The only case that was systematically investigated was that of the 3D SU(2) gauge theory coupled to a scalar SU(2) doublet, which is relevant for the electroweak phase transition (see, e.g., Refs. [28–32]). For our purposes, however, this model is somehow trivial, since it is known that its phase diagram consists of a single phase [33–35].

To improve on this state of affairs, in Ref. [36], we presented results regarding a multiflavor 3D lattice scalar non-Abelian gauge model, which might be called lattice multiflavor scalar chromodynamics. We determined the transitions in this model, investigated their nature, and compared the results with the predictions of two field-theoretical formalisms, the gauge-invariant LGW scheme, and the continuum scalar chromodynamics. The outcome of this analysis was that the LGW approach correctly predicts the finite-temperature critical behavior of 3D multiflavor scalar chromodynamics in all cases we studied, i.e., for $N_c = 2$, 3, 4 and $N_f = 2$, 3. The analysis of the lattice results reported in Ref. [36] was however necessarily sketchy, and in this paper we report all the analyses that permitted us to unambiguously identify the order of the transitions and the universality class in the case of continuous transitions. A more detailed discussion of the interplay between global and gauge symmetries of the model is reported, and in particular the full details of the LGW approach for $N_c = 2$, in which case the global symmetry of the model is $\mathrm{Sp}(N_f)$, and for $N_c \geq 3$ in which the relevant global symmetry is $\mathrm{SU}(N_f)$.

The paper is organized as follows. In Sec. II, the lattice multiflavor scalar chromodynamics model is introduced, with a discussion of its global and local symmetries. In Sec. III, we discuss the predictions of the effective LGW approach. In Sec. IV, we describe the lattice observables adopted and we briefly summarize the finite-size scaling (FSS) results we use in the analysis of the data. In Sec. V, we present the results of the numerical simulations. Finally, we summarize and draw our conclusions in Sec. VI. In Appendix A, we discuss the symplectic order parameters and, for $N_f = 2$, the relation between Sp(2) and O(5) observables. Appendix B is devoted to a discussion of the LGW approach for the two-color case in which the global symmetry group is $\mathrm{Sp}(N_f)$. Finally, in Appendix C, we discuss some properties of the model for $\beta \to \infty$.

II. THE LATTICE MODEL

The three-dimensional lattice model we are going to study has complex $N_c \times N_f$ matrix variables $Z_{\boldsymbol{x}}^{af}$ associated with each site $\boldsymbol{x}$ of a cubic lattice. Our starting point is the lattice model defined by the action

$$S_{\rm inv} = -J \sum_{\boldsymbol{x},\mu} \mathrm{ReTr} Z_{\boldsymbol{x}}^\dagger Z_{\boldsymbol{x}+\hat{\mu}} + \sum_{\boldsymbol{x}} V(\mathrm{Tr} Z_{\boldsymbol{x}}^\dagger Z_{\boldsymbol{x}}), \tag{1}$$

$$V(X) = rX + \frac{1}{2} u X^2, \tag{2}$$

where the first sum is over the lattice links, the second one is over the lattice sites, and $\hat{\mu} = \hat{1}, \hat{2}, \hat{3}$ are unit vectors along the three lattice directions. In particular, we consider the unit-length limit of the site variables, which is formally obtained by setting $r = -u$, and taking the limit $u \to \infty$ in the potential (2), so that the variables Z satisfy

$$\mathrm{Tr} Z_{\boldsymbol{x}}^\dagger Z_{\boldsymbol{x}} = 1, \tag{3}$$

and the action simplifies to

$$S_{\rm inv} = -J \sum_{\boldsymbol{x},\mu} \mathrm{ReTr} Z_{\boldsymbol{x}}^\dagger Z_{\boldsymbol{x}+\hat{\mu}}. \tag{4}$$

Models with actions (1) and (4) are invariant under $\mathrm{O}(M)$ transformations with $M = 2N_c N_f$. This is immediately checked if we write the matrices $Z_{\boldsymbol{x}}$ in terms of M component real vectors $\boldsymbol{S}_{\boldsymbol{x}}$. In the new variables, we obtain the standard $\mathrm{O}(M)$ nonlinear σ model,

$$S_M = -J \sum_{\boldsymbol{x},\mu} \boldsymbol{S}_{\boldsymbol{x}} \cdot \boldsymbol{S}_{\boldsymbol{x}+\hat{\mu}}, \qquad \boldsymbol{S}_{\boldsymbol{x}} \cdot \boldsymbol{S}_{\boldsymbol{x}} = 1. \tag{5}$$

We now proceed by gauging some of the d.o.f. We associate an $\mathrm{SU}(N_c)$ matrix $U_{\boldsymbol{x},\hat{\mu}}$ with each lattice link and extend the action (4) to ensure $\mathrm{SU}(N_c)$ gauge invariance. We also add a kinetic term for the gauge variables in the Wilson form [37]. We obtain the model with action

$$S_g = -\beta N_f \sum_{\boldsymbol{x},\mu} \mathrm{ReTr}[Z_{\boldsymbol{x}}^\dagger U_{\boldsymbol{x},\hat{\mu}} Z_{\boldsymbol{x}+\hat{\mu}}] - \frac{\beta_g}{N_c} \sum_{\boldsymbol{x},\mu>\nu} \mathrm{ReTr}[U_{\boldsymbol{x},\hat{\mu}} U_{\boldsymbol{x}+\hat{\mu},\hat{\nu}} U_{\boldsymbol{x}+\hat{\nu},\hat{\mu}}^\dagger U_{\boldsymbol{x},\hat{\nu}}^\dagger] \tag{6}$$

and partition function

$$Z = \sum_{\{Z,U\}} e^{-S_g}. \tag{7}$$

Note that the gauge group is $\mathrm{SU}(N_c)$ and not $\mathrm{U}(N_c)$, so that, for $N_c = 1$, the model is not related to the 3D CP^{N_f-1} model [9] or to the Abelian Higgs model, studied, e.g., in Ref. [21]. The factor N_f in the first term is introduced so that the large-N_f limit can be performed by keeping β fixed; the factor $1/N_c$ in the second term is instead conventional in the lattice gauge theory literature. Note that, for $\beta_g \to \infty$, the product of

the gauge fields along a plaquette converges to one, and therefore we can set $U_{x,\hat{\mu}} = 1$ modulo a gauge transformation. Therefore, in this limit, we reobtain the O(M) invariant theory (4) we started from.

It is immediate to see that, for any value of N_c and N_f, S_g is invariant under the local gauge transformation

$$Z_x \to G_x Z_x, \qquad U_{x,\hat{\mu}} \to G_x U_{x,\hat{\mu}} G^\dagger_{x+\hat{\mu}}, \tag{8}$$

with $G_x \in \mathrm{SU}(N_c)$, and under the global transformation

$$Z_x \to Z_x V, \qquad U_{x,\hat{\mu}} \to U_{x,\hat{\mu}}, \tag{9}$$

with $V \in U(N_f)$. More precisely, the global symmetry group of the model is $U(N_f)/\mathbb{Z}_{N_c}$, where $\mathbb{Z}_{N_c}$ is the center of the gauge symmetry group $\mathrm{SU}(N_c)$.

Actually, for $N_c = 2$, the action S_g is invariant under a larger global symmetry group, the compact complex symplectic group[1] $\mathrm{Sp}(N_f)$. This is a well-established result (we found mention of it, in various forms, e.g., in Refs. [11,38–40]), which is a consequence of the self-duality of the fundamental representation of SU(2). We will here briefly explain the origin of this symmetry enlargement, introducing also some notations that will be useful in the following.

We define

$$Y^{af}_x = \sum_b \epsilon^{ab} \bar{Z}^{bf}_x, \tag{10}$$

where ϵ^{ab} is the completely antisymmetric tensor in two dimensions ($\epsilon^{12} = -\epsilon^{21} = 1$), and the $2 \times 2N_f$ matrix field $\Gamma^{a\alpha}_x$, defined by

$$\Gamma^{a\alpha}_x = \begin{cases} Z^{a\alpha}_x & \text{if } 1 \le \alpha \le N_f \\ Y^{a(\alpha - N_f)}_x & \text{if } N_f + 1 \le \alpha \le 2N_f \end{cases}. \tag{11}$$

Since SU(2) matrices satisfy

$$\sum_b \epsilon^{ab} \bar{U}^{bc} = \sum_b U^{ab} \epsilon^{bc}, \tag{12}$$

Γ_x transforms covariantly under gauge transformations

$$\Gamma_x \to G_x \Gamma_x. \tag{13}$$

We can now rewrite the nearest-neighbor interaction term involving the scalar variables as

$$\begin{aligned} &\frac{1}{2} \sum_{f,a,b} [\bar{Z}^{af}_x U^{ab}_{x,\hat{\mu}} Z^{bf}_{x+\hat{\mu}} + Z^{af}_x \bar{U}^{ab}_{x,\hat{\mu}} \bar{Z}^{bf}_{x+\hat{\mu}}] \\ &= \frac{1}{2} \sum_{f,a,b} [\bar{Z}^{af}_x U^{ab}_{x,\hat{\mu}} Z^{bf}_{x+\hat{\mu}} + \bar{Y}^{af}_x U^{ab}_{x,\hat{\mu}} Y^{bf}_{x+\hat{\mu}}] \\ &= \frac{1}{2} \sum_{\gamma,a,b} \bar{\Gamma}^{a\gamma}_x U^{ab}_{x,\hat{\mu}} \Gamma^{b\gamma}_{x+\hat{\mu}} = \frac{1}{2} \mathrm{Tr} \Gamma^\dagger_x U_{x,\hat{\mu}} \Gamma_{x+\hat{\mu}}. \end{aligned} \tag{14}$$

Apparently, the action (14) is invariant under the global transformations

$$\Gamma_x \to \Gamma_x M, \qquad M \in \mathrm{U}(2N_f). \tag{15}$$

However, one should bear in mind that the Γ_x variables are not generic, since they are obtained by a formal doubling of the d.o.f. Therefore, one must only consider transformations M that leave the particular structure (11) invariant. To identify them, we note that the previous bipartite structure of Γ is equivalent to the relation

$$\sum_{b=1}^{N_c} \epsilon^{ab} \bar{\Gamma}^{b\alpha}_x = -\sum_{\gamma=1}^{N_f} \Gamma^{a\gamma}_x J^{\gamma\alpha}, \tag{16}$$

where J is the $2N_f \times 2N_f$ matrix

$$J = \begin{pmatrix} 0 & -I \\ I & 0 \end{pmatrix}, \tag{17}$$

and I is the $N_f \times N_f$ identity matrix. Therefore, the global invariance group of S_g is the subgroup of $U(2N_f)$ which leaves invariant the relation Eq. (16). By straightforward manipulations, it is possible to show that this requires M to satisfy

$$MJM^T = J, \tag{18}$$

which identifies the global symmetry group as the compact (unitary) complex symplectic group $\mathrm{Sp}(N_f)$ (see, e.g., Ref. [41]). The global symmetry group for $N_c = 2$ is thus $\mathrm{Sp}(N_f)/\mathbb{Z}_2$, since the sign of the field can be redefined by a gauge transformation. Note that, for $N_f = 2$, we have the isomorphism (see, e.g., Ref. [41])

$$\mathrm{SO}(5) = \mathrm{Sp}(2)/\mathbb{Z}_2. \tag{19}$$

Finally, let us explicitly note that the $\mathrm{Sp}(N_f)$ symmetry also holds when the fields do not satisfy the unit-length condition. Since

$$\mathrm{Tr} Z^\dagger_x Z_x = \frac{1}{2} \mathrm{Tr} \Gamma^\dagger_x \Gamma_x \tag{20}$$

is invariant under any $U(2N_f)$ transformations, and, in particular, under those of its $\mathrm{Sp}(N_f)$ subgroup, the action is

[1]Several notations are used to denote this group: in particular both $\mathrm{Sp}(N_f)$ and $\mathrm{Sp}(2N_f)$ can be found in the literature.

$\mathrm{Sp}(N_f)$ invariant for generic site potentials V in Eqs. (1) and (2).

III. EFFECTIVE FIELD THEORY RESULTS

The critical behavior of the lattice multiflavor scalar chromodynamics was discussed in Ref. [36]. Two different approaches were considered: the continuum scalar chromodynamics corresponding to the lattice model and the LGW Φ^4 theory built in term of a gauge-invariant order parameter.

The renormalization-group flow of multiflavor continuum chromodynamics was studied in the ε expansion around four dimensions [42]. It was found that a stable fixed point only exists for a very large number of flavors [for $N_c = 2$, it exists only for $N_f > 359 + O(\varepsilon)$]. As a consequence, for small values of N_f a first-order transition is predicted.

In the LGW approach, one starts by considering an order parameter that breaks the global symmetry of the model. We first consider the case $N_c > 2$, so that the global symmetry is $U(N_f)/\mathbb{Z}_{N_c}$. Since this is not a simple group, we may have different symmetry breakings.

One possibility is that of breaking the $\mathrm{SU}(N_f)$ subgroup. An appropriate order parameter is the field combination

$$Q_{\boldsymbol{x}}^{fg} = \sum_a \bar{Z}_{\boldsymbol{x}}^{af} Z_{\boldsymbol{x}}^{ag} - \frac{\delta^{fg}}{N_f}, \tag{21}$$

which is the natural generalization of the quantity studied in Abelian models (see, e.g., Refs. [20,21]). The corresponding LGW theory is obtained by considering a Hermitian traceless $N_f \times N_f$ matrix field $\Psi(\boldsymbol{x})$, which represents a coarse-grained version of $Q_{\boldsymbol{x}}$, with Lagrangian

$$\mathcal{L}_{\mathrm{LGW}} = \mathrm{Tr}\partial_\mu\Psi\partial_\mu\Psi + r\mathrm{Tr}\Psi^2 + u_3\mathrm{Tr}\Psi^3 + u_{41}\mathrm{Tr}\Psi^4 + u_{42}(\mathrm{Tr}\Psi^2)^2. \tag{22}$$

This Lagrangian is invariant under the global transformations $\Psi \to V\Psi V^\dagger$, and therefore the symmetry group is $\mathrm{SU}(N_f)/\mathbb{Z}_{N_f}$. As discussed in, e.g., Ref. [20], for $N_f = 2$ the cubic term vanishes and the two quartic terms are equivalent. In this case, a continuous transition is possible in the $\mathrm{SU}(2)/\mathbb{Z}_2$, that is in the O(3) vector, universality class. For $N_f > 2$, the cubic term is present and, on the basis of the usual mean-field arguments, one expects a first-order transition also in three dimensions.

A second possibility is that of breaking the $\mathrm{U}(1)/\mathbb{Z}_{N_c}$ symmetry group associated with the transformations

$$Z_{\boldsymbol{x}}^{af} \to e^{i\alpha} Z_{\boldsymbol{x}}^{af}, \tag{23}$$

which leave invariant the order parameter $Q_{\boldsymbol{x}}^{ab}$. However, for $N_f < N_c$, this additional symmetry is only apparent. Indeed, for any $\boldsymbol{x}$, one can find an $\mathrm{SU}(N_c)$ matrix $G_{\boldsymbol{x}}$ such that

$$e^{i\alpha} Z_{\boldsymbol{x}} = G_{\boldsymbol{x}} Z_{\boldsymbol{x}}. \tag{24}$$

If $N_f < N_c$, there is a gauge transformation $Z'_{\boldsymbol{x}} = G_{1\boldsymbol{x}} Z_{\boldsymbol{x}}$ such that $Z'^{af}_{\boldsymbol{x}} = 0$ for any f and any a satisfying $N_f + 1 \le a \le N_c$. Then, one considers the $N_c \times N_c$ unitary matrix

$$G_2 = \mathrm{diag}(g_1, \ldots, g_{N_c}), \tag{25}$$

with $g_a = e^{i\alpha}$ for $1 \le a \le N_f$, $g_a = e^{-i\alpha N_f}$ for $a = N_f + 1$, $g_a = 1$ for $a > N_f + 1$. It is then easy to verify that $G_x = G_{1\boldsymbol{x}}^\dagger G_2 G_{1\boldsymbol{x}}$ satisfies Eq. (24).

For $N_f \ge N_c$, the relation (24) does not hold anymore, and one should also consider the possibility of a transition characterized by the breaking of the Abelian symmetry $U(1)/\mathbb{Z}_{N_c}$. An appropriate order parameter is

$$D_{\boldsymbol{x}}^{f_1,\ldots,f_{N_c}} = \sum_{a_1,\ldots,a_{N_c}} \epsilon^{a_1,\ldots,a_{N_c}} Z_{\boldsymbol{x}}^{a_1 f_1} \ldots Z_{\boldsymbol{x}}^{a_{N_c} f_{N_c}}, \tag{26}$$

which is invariant under gauge transformations (here $\epsilon^{a_1,\ldots,a_{N_c}}$ is the completely antisymmetric tensor in N_c dimensions). Such an order parameter vanishes for $N_f < N_c$, an expected result given the effective absence of the symmetry in this case. For $N_f = N_c$, the order parameter defined in Eq. (26) is invariant under $\mathrm{SU}(N_f)$ transformations and therefore it is a good order parameter for the breaking of the U(1) flavor symmetry. It can be rewritten in a simpler way as

$$D_{\boldsymbol{x}}^{f_1,\ldots,f_{N_c}} = \epsilon^{f_1,\ldots,f_{N_c}} \det Z_{\boldsymbol{x}}. \tag{27}$$

On the other hand, for $N_f > N_c$, the order parameter belongs to a nontrivial representation of $\mathrm{SU}(N_f)$. Therefore, it condenses only if both the $\mathrm{SU}(N_f)$ and the U(1) symmetries are broken. As we discuss in Appendix C, in our model, for $N_c \ge 3$, the order parameter $D_{\boldsymbol{x}}^{f_1,\ldots,f_{N_c}}$ vanishes for $\beta \to \infty$. If we assume that the relevant configurations in the low-temperature phase are simply obtained by considering short-range fluctuations on top of the ordered background observed for $\beta = +\infty$, we conclude that D correlations are short ranged in the low-temperature phase, i.e., that the U(1) symmetry is not broken. Below we will present numerical results for $N_c = N_f = 3$ that confirm this picture.

For $N_c = 2$, the symmetry group is $\mathrm{Sp}(N_f)/\mathbb{Z}_2$. The order parameter is a symplectic analog of $Q_{\boldsymbol{x}}$. Specifically, we define

TABLE I. Summary of the predictions of the LGW approach for the nature and universality class of the finite-temperature transition of the scalar chromodynamics defined by the action (6). For $N_c \geq 3$ and $N_f \geq N_c$, we have assumed that the flavor U(1) symmetry does not play any role.

Flavors	Colors	Universality class
$N_f = 2$	$N_c = 2$	O(5) vector
$N_f = 2$	$N_c \geq 3$	O(3) vector
$N_f \geq 3$	$N_c \geq 2$	first order

$$\mathcal{T}_{\boldsymbol{x}}^{\alpha\beta} = \sum_a \bar{\Gamma}_{\boldsymbol{x}}^{a\alpha}\Gamma_{\boldsymbol{x}}^{a\beta} - \frac{\delta^{\alpha\beta}}{2N_f}\sum_{a\gamma}\bar{\Gamma}_{\boldsymbol{x}}^{a\gamma}\Gamma_{\boldsymbol{x}}^{a\gamma}, \tag{28}$$

with $\Gamma_{\boldsymbol{x}}^{a\alpha}$ defined in Eq. (11). This order parameter is a $2N_f \times 2N_f$ Hermitian traceless matrix which satisfies the additional condition

$$J\bar{\mathcal{T}}J + \mathcal{T} = 0, \tag{29}$$

which follows from Eq. (16). The matrix $\mathcal{T}$ is thus an element of the $\mathfrak{sp}(N_f)$ algebra [41]. The explicit construction of the corresponding LGW theory starts by defining a $2N_f \times 2N_f$ Hermitian traceless matrix field $\Psi(\boldsymbol{x})$ that satisfies the analog of Eq. (29). The corresponding LGW theory is obtained by considering the most general quartic polynomial in the fields: we reobtain Eq. (22). For $N_f = 2$, as discussed in Appendix B, the cubic term vanishes and the two quartic terms are equivalent. Therefore, continuous transitions are allowed in the O(5) vector universality class, given the isomorphism between $\mathrm{Sp}(2)/\mathbb{Z}_2$ and the SO(5) group. For $N_f > 2$, a cubic operator is generically present and therefore we expect first-order transitions. Note, that for $N_c = 2$, there is no residual U(1) symmetry, as U(1) global transformations are a subgroup of the $\mathrm{Sp}(N_f)$ group.

We finally note that the LGW approach based on the symmetry of the model does not depend on the specific form of the lattice O(M)-invariant potential $V(X)$ in Eq. (2). Moreover, we recall that the presence of a stable fixed point in the corresponding LGW theory does not exclude the possibility that the model undergoes a first-order transition, when the system is outside the attraction domain of the stable fixed point, even though it shares the global symmetry of the universality class.

Table I reports a summary of the predictions based on the LGW approach, assuming that the critical behavior is determined by the global symmetry group and that the gauge d.o.f. are irrelevant.

IV. OBSERVABLES AND ANALYSIS METHOD

In this section, we introduce the lattice observables studied and we briefly recall some basic facts about FSS that will be relevant for the analysis of the numerical data. We always assume the lattice to have periodic boundary conditions and to be of linear size L.

A. Lattice observables

In the following, we consider the energy density and the specific heat defined as

$$E = \frac{1}{\beta N_f V}\langle S_g\rangle, \qquad C = \frac{1}{\beta^2 N_f^2 V}(\langle S_g^2\rangle - \langle S_g\rangle^2), \tag{30}$$

where $V = L^3$. We also define the average gauge energy as

$$E_g = \frac{1}{6VN_c}\left\langle \sum_{\boldsymbol{x},\mu>\nu} \mathrm{ReTr}[U_{\boldsymbol{x},\hat{\mu}}U_{\boldsymbol{x}+\hat{\mu},\hat{\nu}}U^\dagger_{\boldsymbol{x}+\hat{\nu},\hat{\mu}}U^\dagger_{\boldsymbol{x},\hat{\nu}}]\right\rangle. \tag{31}$$

To study the breaking of the $\mathrm{SU}(N_f)$ flavor symmetry, we consider the order parameter Q defined in Eq. (21), which is a Hermitian and traceless $N_f \times N_f$ matrix. Its two-point correlation function is defined by

$$G(\boldsymbol{x}-\boldsymbol{y}) = \langle \mathrm{Tr}Q_{\boldsymbol{x}}Q_{\boldsymbol{y}}\rangle, \tag{32}$$

where the translation invariance of the system has been explicitly taken into account. We define the corresponding susceptibility χ and correlation length ξ as

$$\chi = \sum_{\boldsymbol{x}} G(\boldsymbol{x}), \tag{33}$$

$$\xi^2 = \frac{1}{4\sin^2(\pi/L)}\frac{\tilde{G}(\boldsymbol{0}) - \tilde{G}(\boldsymbol{p}_m)}{\tilde{G}(\boldsymbol{p}_m)}, \tag{34}$$

where $\tilde{G}(\boldsymbol{p}) = \sum_{\boldsymbol{x}} e^{i\boldsymbol{p}\cdot\boldsymbol{x}}G(\boldsymbol{x})$ is the Fourier transform of $G(\boldsymbol{x})$ and $\boldsymbol{p}_m = (2\pi/L, 0, 0)$. We also consider the Binder parameter U defined by

$$U = \frac{\langle \mu_2^2\rangle}{\langle \mu_2\rangle^2}, \qquad \mu_2 = \frac{1}{V^2}\sum_{\boldsymbol{x},\boldsymbol{y}}\mathrm{Tr}Q_{\boldsymbol{x}}Q_{\boldsymbol{y}}. \tag{35}$$

We also study the residual U(1) flavor symmetry, only for $N_f = N_c$. For this purpose, we consider the scalar order parameter, see Eq. (27),

$$D_{\boldsymbol{x}} = \det Z_{\boldsymbol{x}}. \tag{36}$$

We define the correlation function

$$G_D(\boldsymbol{x}-\boldsymbol{y}) = \langle \mathrm{Re}\bar{D}_{\boldsymbol{x}}D_{\boldsymbol{y}}\rangle, \tag{37}$$

the correlation length ξ_D using the analogue of Eq. (34), and the Binder parameter

$$U_D = \frac{\langle \mu_{D2}^2 \rangle}{\langle \mu_{D2} \rangle^2}, \qquad \mu_{D2} = \frac{1}{V^2} \sum_{x,y} \mathrm{Re} \bar{D}_x D_y. \tag{38}$$

To better appreciate the role of the gauge d.o.f., we also study some observables involving the $\mathrm{SU}(N_c)$ gauge link variables. More specifically, we consider the averages

$$\left\langle \sum_{ab} \bar{Z}_x^{af} \left[\prod_{\ell \in \mathcal{C}} U_\ell \right]^{ab} Z_y^{bg} \right\rangle, \tag{39}$$

where the product extends over the link variables that belong to a lattice path $\mathcal{C}$ connecting the points $\boldsymbol{x}$ and $\boldsymbol{y}$. To define quantities that have the correct FSS, the path $\mathcal{C}$ must be chosen appropriately [43], and here we consider correlations between points along lattice lines,

$$G_V(t,L) = \mathrm{Re} \left\langle \sum_{abfg} \bar{Z}_x^{af} \left[\prod_{k=0}^{t-1} U_{x+k\hat{\mu},\hat{\mu}} \right]^{ab} Z_{x+t\hat{\mu}}^{bf} \right\rangle. \tag{40}$$

As usual, translation invariance and independence of the direction $\hat{\mu}$ can be used to actually increase the statistics. In some test cases, we also determined the Polyakov loop

$$P(L) = \frac{1}{3L^3} \sum_{x,\mu} \mathrm{Re} \left\langle \mathrm{Tr} \left[\prod_{k=0}^{L-1} U_{x+k\hat{\mu},\hat{\mu}} \right] \right\rangle. \tag{41}$$

For $N_f = 2$ and $N_c = 2$, the model is invariant under $\mathrm{Sp}(2)/\mathbb{Z}_2 = \mathrm{SO}(5)$ transformations. We discuss in Appendix A the O(5) observables that can be defined in terms of the order parameter (28). In particular, we show that the second-moment correlation length computed from $G(\boldsymbol{x})$, $G_D(\boldsymbol{x})$ or the O(5)-invariant correlation function of the order parameter $\mathcal{T}^{\alpha\beta}$ are numerically the same. For the Binder parameters, instead, the relation is not trivial. We have

$$U = \frac{25}{21} U_\Gamma, \qquad U_D = \frac{10}{7} U_\Gamma, \tag{42}$$

where U_Γ is the O(5)-invariant Binder parameter defined in Appendix A, which corresponds to the usual vector parameter in the O(5) vector theory.

For $N_f = 2$ and $N_c \geq 3$, the global symmetry group is $\mathrm{SU}(2)/\mathbb{Z}_2 = \mathrm{SO}(3)$. This invariance can be more easily understood by defining the gauge-invariant three-component real vector variables φ_x^k as

$$\varphi_x^k = \sum_{a,f,g} \bar{Z}_x^{af} \sigma_{fg}^k Z_x^{ag} = \sum_{f,g} \sigma_{fg}^k Q_x^{fg}, \tag{43}$$

where σ^k are the Pauli matrices. Previously defined observables, like χ and U, can be rewritten in term of the vector variable $\boldsymbol{\varphi}_x$ using

$$G(\boldsymbol{x}-\boldsymbol{y}) = \frac{1}{2} \langle \boldsymbol{\varphi}_x \cdot \boldsymbol{\varphi}_y \rangle, \tag{44}$$

$$U = \frac{\langle \mu_2^2 \rangle}{\langle \mu_2 \rangle^2}, \qquad \mu_2 = \frac{1}{V^2} \sum_{x,y} \boldsymbol{\varphi}_x \cdot \boldsymbol{\varphi}_y. \tag{45}$$

Note however that the vectors $\boldsymbol{\varphi}_x$ do not have fixed length; indeed

$$\boldsymbol{\varphi}_x \cdot \boldsymbol{\varphi}_x = 2\mathrm{Tr} Q_x^2 \leq 1. \tag{46}$$

B. Finite-size scaling

To investigate continuous transitions using FSS, it is particularly convenient to study RG invariant quantities, such as U and

$$R_\xi = \xi/L. \tag{47}$$

For RG-invariant quantities, generically denoted by R, FSS theory predicts the scaling behavior [8]

$$R(\beta,L) = f_R(X) + L^{-\omega} g_R(X) + \cdots, \tag{48}$$

$$X = (\beta - \beta_c) L^{1/\nu}, \tag{49}$$

where $f_R(X)$ is a function that is universal up to a multiplicative scale of its argument, ν is the critical exponent associated with the correlation length, and ω is the exponent associated with the leading irrelevant operator. By expanding Eq. (48) around β_c, corresponding to $X = 0$, we can write

$$R(\beta,L) \approx R^* + \sum_{k=1}^{n} a_k X^k + L^{-\omega} \sum_{k=0}^{m} b_k X^k, \tag{50}$$

where, as in Eq. (48), we have neglected next-to-leading scaling corrections. Using this expression, it is possible to estimate β_c and ν from numerical determinations of R.

Since R_ξ defined in Eq. (47) is an increasing function of β, we may write

$$U(\beta,L) = F_U(R_\xi) + O(L^{-\omega}), \tag{51}$$

where F_U now depends on the universality class only, without any nonuniversal multiplicative factor. This is true once the boundary conditions and the shape of the lattice have been fixed, and provided one uses corresponding quantities in the different models; see, e.g., Ref. [20] and the discussion in Sec. V A. The scaling (51) is particularly convenient to test universality-class predictions, since it permits easy comparisons between different models without tuning nonuniversal parameters.

Finally, we also mention that the susceptibility is expected to scale as [8]

$$\chi(\beta, L) \approx L^{2-\eta}[f_\chi(X) + L^{-\omega} g_\chi(X)] \tag{52}$$

$$= L^{2-\eta}[F_\chi(R_\xi) + O(L^{-\omega})], \tag{53}$$

where f_χ and F_χ are universal functions, apart from trivial multiplicative normalizations and a normalization of the argument in the case of f_χ.

V. NUMERICAL RESULTS

We now present and discuss the results of Monte Carlo (MC) simulations. We use an overrelaxation algorithm, consisting of a combination of heat-bath [44,45] and microcanonical [46] updates (with ratio 1:5) for the gauge fields (implemented *à la* Cabibbo-Marinari [47] for $N_c > 2$) and of a combination of Metropolis [48] and microcanonical updates for the scalar field. The Metropolis update was tuned to have an acceptance rate of approximately 30%.

A. FSS analysis for $N_f = 2$ and $N_c = 2$

In this section, we present the numerical results obtained for $N_f = 2$ and $N_c = 2$. We start by analyzing the computationally simplest case $\beta_g = 0$. In this case, we performed simulations on lattices of size up to $L = 96$.

In Fig. 1, we show the estimates of R_ξ for different values of L and β. They display the typical behavior expected at a continuous transition: different curves have an approximate crossing point and the slopes increase by increasing the lattice size. Equation (50) can then be used to extract the critical coupling β_c and the critical exponent ν. For this purpose, we first perform standard nonlinear (unbiased) fits to the ansatz,

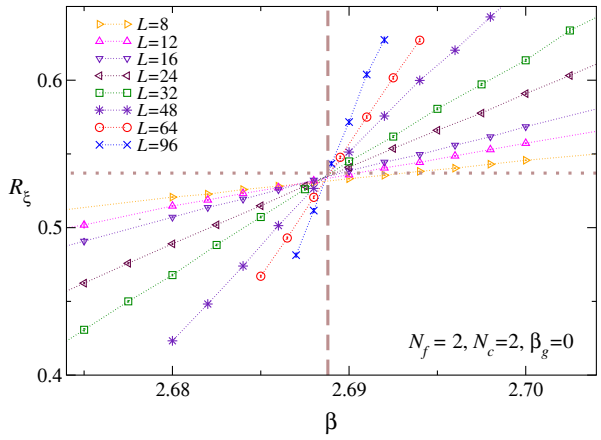

FIG. 1. R_ξ versus β for $N_f = 2$, $N_c = 2$, and $\beta_g = 0$. The data for different values of L have a crossing point, whose position provides an estimate of the critical point, $\beta_c = 2.68885(5)$, indicated by the vertical line. The horizontal line corresponds to the universal value $R_\xi^* = 0.538(1)$ for the O(5) vector universality class.

TABLE II. Results of the biased fits of R_ξ to the ansatz (50) with $n = 1$, $m = 0$, fixing ν and ω to the O(5) universal values reported in Eq. (55). Results for $N_c = N_f = 2$ and $\beta_g = 0$.

δ	$L_{\min}$	β_c	R_ξ^*	χ^2/d.o.f.	# data
0.05	8	2.68886(3)	0.5381(3)	1.1	45
0.10	8	2.68887(2)	0.5378(3)	1.4	68
0.05	12	2.68880(4)	0.5372(6)	1.1	33
0.10	12	2.68880(3)	0.5364(5)	1.4	52
0.05	24	2.68886(8)	0.539(3)	1.2	13
0.10	24	2.68884(6)	0.538(2)	1.3	26

$$R_\xi = R_\xi^* + a_1 X, \qquad X = (\beta - \beta_c) L^{1/\nu}, \tag{54}$$

using data within the self-consistent window $R_\xi(\beta, L) \in [R_\xi^*(1-\delta), R_\xi^*(1+\delta)]$. For $\delta = 0.1$ and $L \geq L_{\min} = 16$, we obtain $\beta_c = 2.68869(2)$, $\nu = 0.775(6)$, and $R_\xi^* = 0.5340(2)$, with χ^2/d.o.f. ≈ 1.5 (30 data, d.o.f. is the number of d.o.f. of the fit). The exponent ν is consistent with that of the O(5) vector universality class, whose universal critical exponents are [49–52]

$$\nu = 0.779(3), \qquad \eta = 0.034(1), \qquad \omega = 0.79(2). \tag{55}$$

To corroborate this identification, we perform biased fits to Eq. (50), with $n = 1$ and $m = 0$ (we include a single scaling correction term), fixing ν and ω to the O(5) universal values reported in Eq. (55). Again, we use a self-consistent fit window $R_\xi(\beta, L) \in [R_\xi^*(1-\delta), R_\xi^*(1+\delta)]$. The results are reported in Table II. Our final biased estimates, that take into account the dependence of the fit parameters on δ and $L_{\min}$, are

$$\beta_c = 2.68885(5), \qquad R_\xi^* = 0.538(2). \tag{56}$$

The errors also take into account the variation of the estimates as ν and ω vary within one error bar. The corresponding scaling plot is shown in Fig. 2, where R_ξ is plotted versus $X = (\beta - \beta_c) L^{1/\nu}$ using $\beta_c = 2.68885$ and the O(5) value $\nu = 0.779$. The agreement is excellent. Note also that the estimate of R_ξ^* is consistent with $R_\xi^* = 0.538(1)$, obtained in the O(5) vector model using the vector correlation function [50]. Also, the behavior of the susceptibility χ is consistent with a transition in the O(5) universality class. If we fix η to the O(5) value [see Eq. (55)], the ratio $\chi/L^{2-\eta}$ scales nicely when plotted versus R_ξ, as expected from the scaling relation Eq. (53); see Fig. 3.

Additional evidence that the transition belongs to the O(5) vector universality class is provided by the analysis of the Binder parameter U defined in Eq. (35). To perform the correct universality check, we should compare

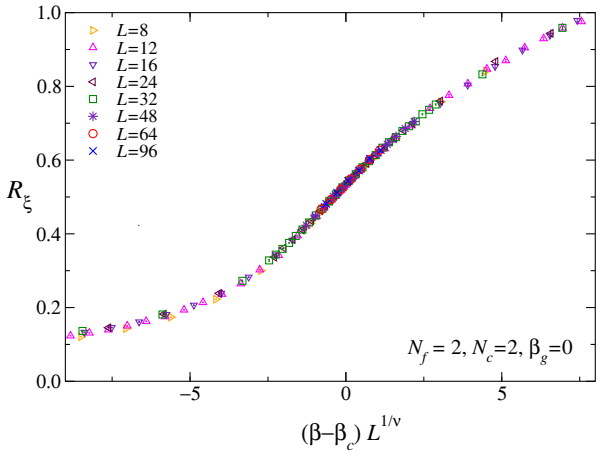

FIG. 2. R_ξ versus $(\beta - \beta_c)L^{1/\nu}$ for $N_f = 2$, $N_c = 2$, and $\beta_g = 0$. We use $\beta_c = 2.68885$ and $\nu = 0.779$, the estimate of the correlation-length exponent for the O(5) vector universality class, see Ref. [50].

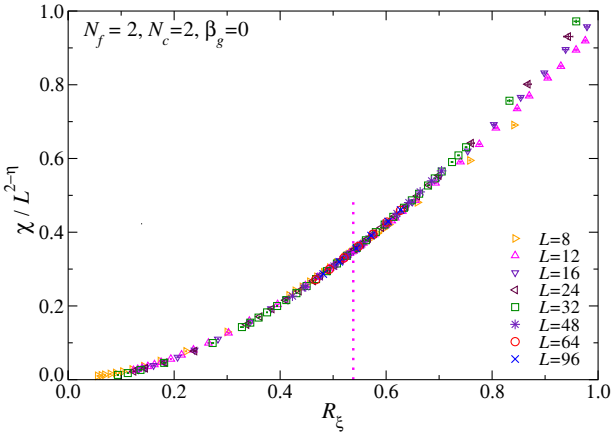

FIG. 3. Rescaled susceptibility $\chi/L^{2-\eta}$ versus R_ξ, for $N_f = 2$, $N_c = 2$, and $\beta_g = 0$. We use the estimate $\eta = 0.034$, the estimate for the O(5) vector universality class; see Ref. [50]. The dotted vertical line corresponds to the critical value R_ξ^* for the O(5) vector universality class.

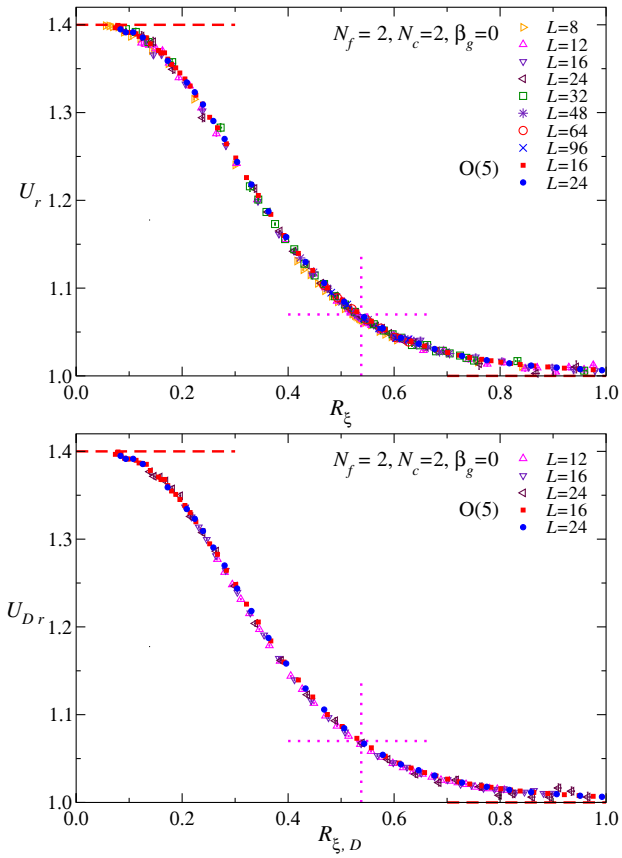

FIG. 4. Rescaled Binder parameter U_r versus R_ξ (top) and rescaled Binder parameter U_{Dr} versus $R_{\xi,D} = \xi_D/L$ (bottom). Results for $N_f = 2$, $N_c = 2$, and $\beta_g = 0$. Data are in good agreement with the numerical results for the Binder parameter obtained by numerical simulations of the lattice O(5) vector model. The dotted horizontal and vertical lines correspond to the universal values $U^* = 1.069(1)$ and $R_\xi^* = 0.538(1)$ of the O(5) vector universality class. The dashed horizontal lines correspond to $U_r = 7/5$ and $U_r = 1$, the asymptotic values for $R_\xi \to 0$ and for $R_\xi \to \infty$, respectively.

corresponding quantities in our model and in the O(5) vector model. As we discuss at length in Appendix A, the Binder parameter that corresponds to the O(5) parameter is U_Γ defined by using $\mathcal{T}^{\alpha\beta}$; see Eq. (A8). Using the Sp(2) or O(5) invariance of the theory, one can easily show that U_Γ and U simply differ by a multiplicative constant; see Eq. (A15). Therefore, the renormalized Binder parameter

$$U_r = \frac{21}{25} U \tag{57}$$

should behave as the vector Binder parameter in the O(5) vector model. If we perform biased fits to Eq. (50) analogous to those we performed for R_ξ, we obtain $U_r^* = 1.070(1)$, which is in agreement with the O(5) estimate $U^*_{\mathrm{O}(5)} = 1.069(1)$ reported in Ref. [50]. A conclusive evidence for an O(5) critical behavior is provided by Fig. 4, where we report U_r versus R_ξ (upper panel). The numerical data fall on top of those obtained in the O(5) vector model.

As we discussed in Sec. III, in the models with $N_c = 2$ the U(1) flavor symmetry breaks at the same β where the $\mathrm{SU}(N_f)$ is broken, since the two groups are subgroups of the larger symmetry group $\mathrm{Sp}(N_f)$. To verify this point, we have estimated several observables in terms of the order parameter D_x defined in Eq. (36). We have verified that the correlation length ξ_D defined using the correlation function (37) is identical, within errors, to ξ. Moreover, we have studied the behavior of the Binder parameter U_D. Again, to obtain a quantity that can be directly related to the O(5) Binder parameter, we have considered, see Eq. (A15),

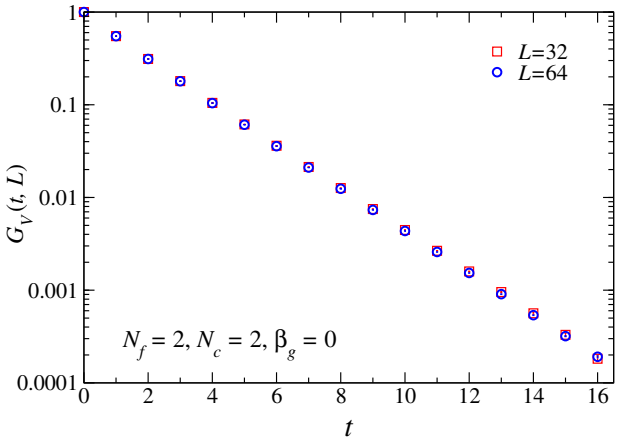

FIG. 5. The correlation function G_V defined in Eq. (40), for $N_f = 2$, $N_c = 2$, and $\beta_g = 0$ at β_c. It shows a large-distance exponential behavior $\sim e^{-x/\xi_g}$ with $\xi_g = 1.92(2)$.

$$U_{Dr} = \frac{7}{10} U_D. \tag{58}$$

In Fig. 4 (lower panel), we report U_{Dr} versus $R_{\xi,D} = \xi_D/L$. The data are compared with the O(5) corresponding data, observing again an excellent agreement.

Finally, we have computed the correlation function $G_V(t)$, defined in Eq. (40). As it is evident from Fig. 5, it is short ranged and essentially independent of L even at the critical point. It has a very clear exponential behavior, $G_V(t) \sim \exp(-x/\xi_g)$, with $\xi_g = 1.92(2)$, independently of the size L. We also analyzed the Polyakov loop which is expected to behave as e^{-L/ξ_P}. The estimates of ξ_P are close to those of ξ_g, but with significantly larger errors.

We have also verified that analogous results are obtained for $\beta_g \neq 0$. For this purpose, we performed MC simulations at $\beta_g = -2$ (using lattices up to $L = 32$) and at $\beta_g = 2$ (using lattices up to $L = 48$). In both cases, data fully support the presence of a continuous transition in the O(5) vector universality class. As an example, in Fig. 6, we plot U_r versus R_ξ for $\beta_g = 2$. Again, the data fall on top of the corresponding ones obtained in the O(5) vector model. Biased fits to Eq. (50) allow us to obtain the estimates $\beta_c(\beta_g = -2) = 3.794(2)$ and $\beta_c(\beta_g = 2) = 1.767(1)$. While the critical coupling at $\beta_g = 2$ is significantly lower than the value $\beta_c(\beta_g = 0) \approx 2.689$, it is still quite larger than the value $\beta_c = 0.96339(1)$ which is attained in the limit of large β_g, when the model become equivalent to the O(8) vector model [53]. This could explain the absence of significant crossover effects in our data induced by the unstable $O(2N_fN_c)$ fixed point at $\beta_g \to \infty$, which have instead been observed in the Abelian case [21]. We finally note that the approach to the asymptotic scaling behavior is significantly slower for $\beta_g = 2$ than for $\beta_g = 0$; see Fig. 6. This is likely related to the fact that the gauge length scale ξ_g at the transition is larger at $\beta_g = 2$ than at $\beta_g = 0$. Indeed,

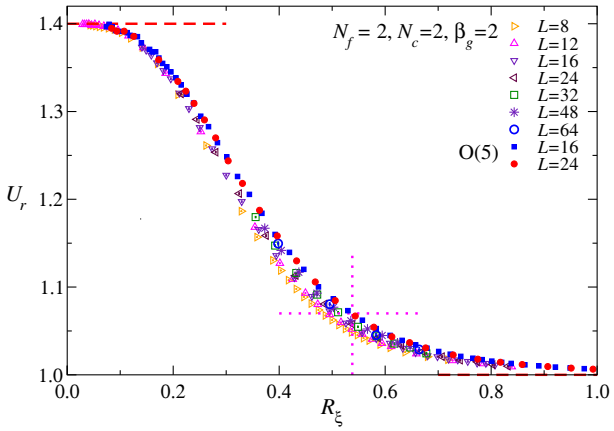

FIG. 6. Estimates of the rescaled Binder parameter U_r versus R_ξ, for $N_f = 2$, $N_c = 2$, and $\beta_g = 2$, and of the usual Binder parameter for the O(5) vector model. The dotted horizontal and vertical lines indicate the universal values $U^* = 1.069(1)$ and $R_\xi^* = 0.538(1)$ of the O(5) universality class. The dashed horizontal lines correspond to the asymptotic values $U_r = 7/5$ and $U_r = 1$ for $R_\xi \to 0$ and $R_\xi \to \infty$, respectively.

we find $\xi_g(\beta_g = 2) = 2.46(4)$, to be compared with $\xi_g(\beta_g = 0) = 1.92(2)$.

The above results provide a robust evidence that the lattice scalar chromodynamics for $N_f = 2$ and $N_c = 2$ undergoes a continuous transition in the O(5) vector universality class. This result agrees with the predictions of the LGW approach, assuming that the critical behavior is determined by the global symmetry group and that the gauge d.o.f. are irrelevant.

We have shown that the same universal behavior emerges in a large interval of values of β_g around $\beta_g = 0$. We predict the same behavior for all positive finite values of β_g. However, for $\beta_g \to \infty$, we expect a crossover to the O(8) critical behavior. The behavior for large negative values of β_g is less clear, since the large frustration arising in the $\beta_g \to -\infty$ limit may give rise to a change of the nature of the transition. This issue requires further investigation.

B. FSS analysis for $N_f = 2$ and $N_c = 3,4$

In this section, we consider the model for $N_f = 2$ and $N_c = 3$, 4. For $N_c = 3$ and $\beta_g = 0$, we have performed simulations up to $L = 64$. In Fig. 7, we report R_ξ as a function of β. We observe a crossing point for $\beta \approx 3.75$. To determine the nature of the transition, we again proceed by first performing standard nonlinear (unbiased) FSS fits of the R_ξ data to the simplest ansatz Eq. (54), using data within the self-consistent window $R_\xi(\beta, L) \in [R_\xi^*(1-\delta), R_\xi^*(1+\delta)]$. For $\delta = 0.1$ and $L \geq L_{\min} = 8$, we obtain $\beta_c = 3.7523(1)$, $\nu = 0.705(10)$, and $R_\xi^* = 0.5771(5)$, with $\chi^2/\text{d.o.f.} \approx 1.4$ (28 data). The critical exponent ν is consistent with that of the O(3) vector universality class, as

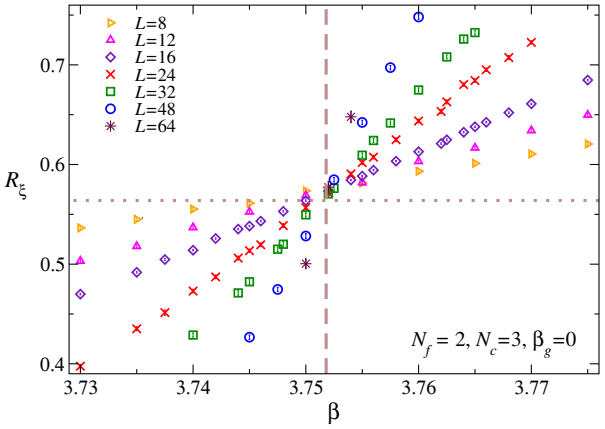

FIG. 7. R_ξ versus β for $N_f = 2$, $N_c = 3$, and $\beta_g = 0$. The data for different values of L show a crossing point, whose position provides an estimate of the critical point, $\beta_c = 3.7518(2)$, indicated by the vertical line. The horizontal line corresponds to the universal value $R_\xi^* = 0.5639(2)$ of the O(3) vector universality class.

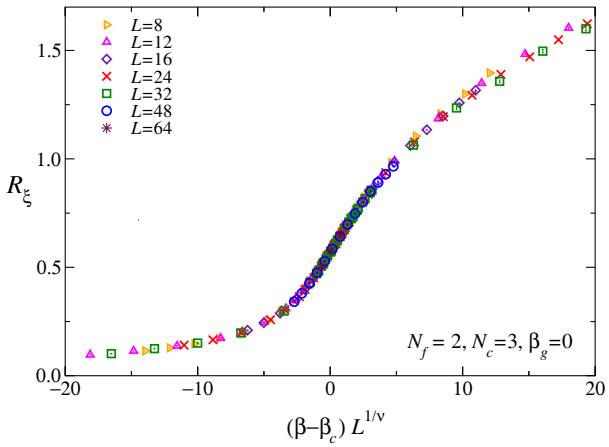

FIG. 8. R_ξ versus $(\beta - \beta_c)L^{1/\nu}$ for $N_f = 2$, $N_c = 3$, and $\beta_g = 0$. We use $\beta_c = 3.7518$ and $\nu = 0.7117$, the correlation-length exponent for the O(3) vector universality class.

predicted by the LGW theory. The universal critical exponents and RG invariant quantities of the O(3) vector universality class which are relevant for our study are [54–56]

$$\nu = 0.7117(5), \quad \eta = 0.0378(3), \quad \omega = 0.782(13), \tag{59}$$

$$R_\xi^* = 0.5639(2), \qquad U^* = 1.1394(3). \tag{60}$$

Additional evidence for a O(3) critical behavior is obtained by performing biased fits to Eq. (50) with $n = 1$ and $m = 0$, fixing ν and ω to the O(3) values reported in Eq. (59). As before, we use data within the self-consistent window $R_\xi(\beta, L) \in [R_\xi^*(1-\delta), R_\xi^*(1+\delta)]$. The results are reported in Table III. The estimates of R_ξ^* are nicely consistent with the O(3) estimate $R_\xi^* = 0.5639(2)$. A similar analysis can be done using the Binder parameter U. Using $L_{\min} = 8$, we obtain the estimates $\beta_c = 3.7519(2)$ and $U^* = 1.139(3)$, with $\chi^2/\text{d.o.f} \approx 1.2$ (27 data). Again, the estimate of U^* is in good agreement with the O(3) value $U^* = 1.1394(3)$. Our final estimate of the critical temperature, obtained by considering the various systematic errors, is

$$\beta_c = 3.7518(2). \tag{61}$$

In Figs. 8–10, we show different scaling plots that clearly confirm that the transition belongs to the O(3) vector universality class. In particular, the data of U plotted versus R_ξ, see Fig. 9, are nicely consistent with the results obtained in numerical simulations of the O(3) vector model.

As in the two-color case, we have also checked that the above results extend to nonvanishing values of β_g. In particular, simulations have been performed for a few values of β_g between -9 and 6. In all cases, the FSS

TABLE III. Results of the biased fits for R_ξ to Eq. (50) with $n = 1$ and $m = 2$, fixing ν and ω to the O(3) values reported in Eq. (59). Results for $N_f = 2$, $N_c = 3$, and $\beta_g = 0$.

δ	$L_{\min}$	β_c	R_ξ^*	χ^2/d.o.f.	# data
0.1	8	3.75182(9)	0.5673(12)	1.1	27
0.1	12	3.75186(16)	0.569(4)	1.2	20
0.1	24	3.7521(4)	0.577(16)	0.8	30
0.1	32	3.7519(11)	0.57(6)	0.6	17

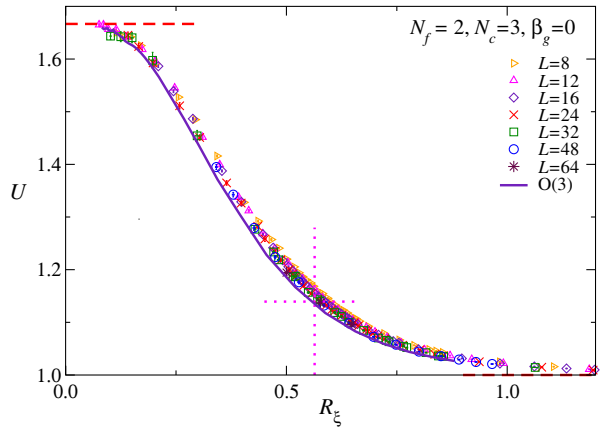

FIG. 9. The Binder parameter U versus R_ξ, for $N_f = 2$, $N_c = 3$, and $\beta_g = 0$. The data clearly converge to the O(3) vector universal curve (continuous curve). The dotted horizontal and vertical lines correspond to the universal values $U^* = 1.1394(3)$ and $R_\xi^* = 0.5639(2)$ of the O(3) universality class. The dashed horizontal lines correspond to $U = 5/3$ and $U = 1$, the asymptotic values of $R_\xi \to 0$ and for $R_\xi \to \infty$, respectively.

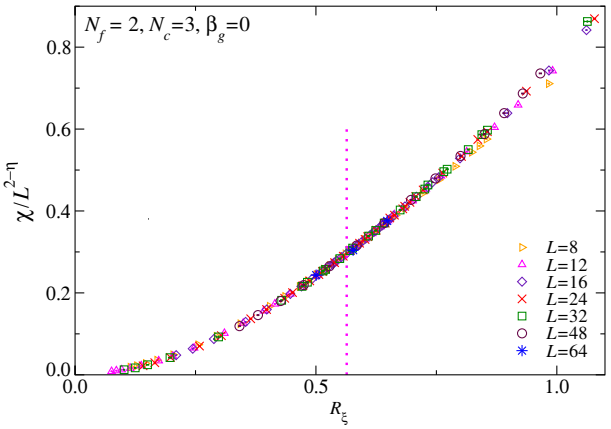

FIG. 10. The rescaled susceptibility $\chi/L^{2-\eta}$ with $\eta = 0.0378$, the exponent value in the O(3) vector universality class, versus R_ξ, for $N_f = 2$, $N_c = 3$, and $\beta_g = 0$. The dotted vertical line corresponds to R_ξ^*.

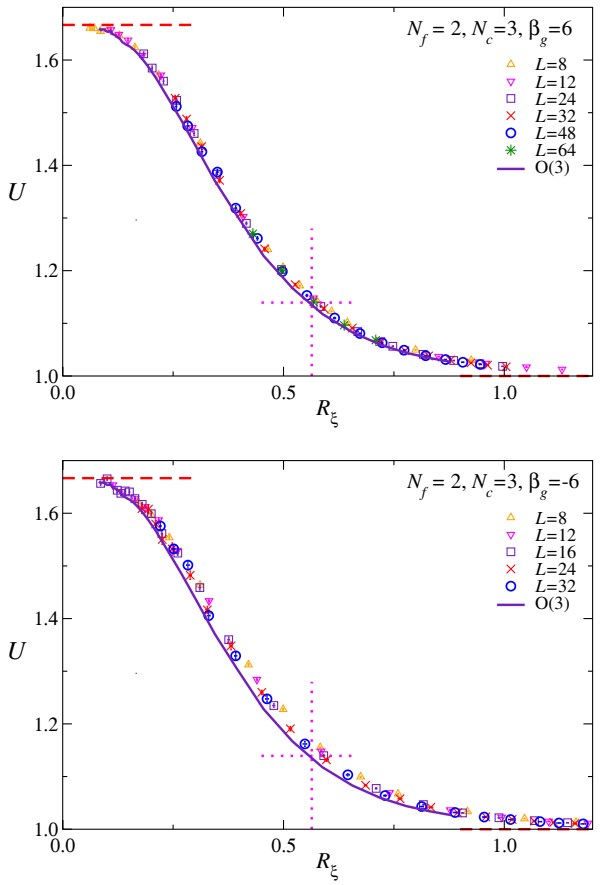

FIG. 11. The Binder parameter U versus R_ξ for $N_f = 2$, $N_c = 3$. In the lower panel, we report results for $\beta_g = -6$ up to $L = 32$, in the upper panel results for $\beta_g = 6$ up to $L = 64$. The data appear to converge to the O(3) vector universal curve (continuous line). The dotted horizontal and vertical lines correspond to the universal values $U^* = 1.1394(3)$ and $R_\xi^* = 0.5639(2)$ of the O(3) universality class. The dashed horizontal lines correspond to $U = 5/3$ and $U = 1$, the asymptotic values for $R_\xi \to 0$ and $R_\xi \to \infty$.

behavior of U as a function of R_ξ supports the O(3) nature of the transition, as can be seen in Fig. 11, where we report the results for $\beta_g = -6$ and $\beta_g = 6$. Again these results are far from trivial, since the critical coupling $\beta_c(\beta_g)$ changes from approximately 4.39 to 2.55 as we vary β_g in the interval $[-9, 6]$ (see Fig. 12). Therefore, the effect of β_g on the dynamics of the system is large. Also, the average gauge energy E_g at criticality changes significantly. It varies approximately from -0.23 to 0.51. These values are however still far from the asymptotic values for $\beta_g \to \pm\infty$. In particular, for positive β_g, the significant difference between our estimate $E_g \approx 0.51$ for $\beta_g = 6$ and $E_g = 1$, the result for $\beta_g \to \infty$, could explain the absence of sizable crossover effects in our data, due to the $O(M)$ fixed point that controls the critical behavior for $\beta_g = \infty$. This is also consistent with the fact that the correlation length associated with the gauge modes increases with increasing β_g, but nevertheless is quite small: at the transition we obtain $\xi_g(\beta_g = 0) = 1.60(2)$, $\xi_g(\beta_g = 3) = 1.70(2)$, and $\xi_g(\beta_g = 6) = 2.02(2)$.

As a final check that, for $N_f = 2$ and any $N_c \geq 3$, the transition always belongs to the O(3) vector universality class, we performed MC simulations for $N_c = 4$ and $\beta_g = 0$. Also, in this case, the data of U plotted versus R_ξ (we have results for $L \leq 48$) clearly approach the O(3) curve as L is increased, as it can be seen in Fig. 13. Again, the results confirm the LGW predictions. Concerning the range of validity of these conclusions with respect to variation of the plaquette coupling β_g, the same remarks reported at the end of Sec. V A apply here as well.

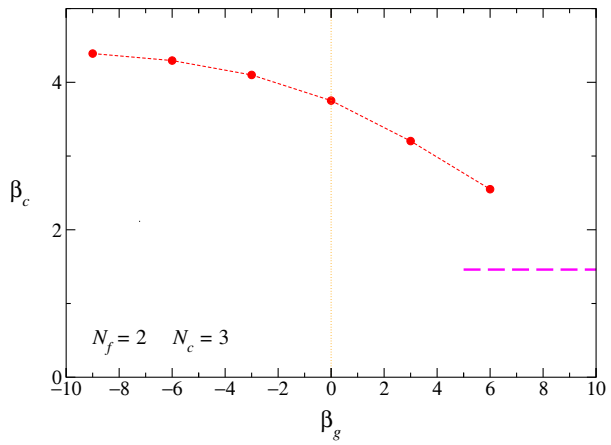

FIG. 12. Estimates of β_c versus β_g for the model with $N_f = 2$, $N_c = 3$. In all cases, the critical behavior belongs to the O(3) vector universality class. The dashed line indicates the critical value in the limit $\beta_g \to \infty$, corresponding to the critical point of the O(12) vector theory, $\beta_c \approx 1.46$, obtained using the results reported in Ref. [57]. The dotted line connecting the data is drawn to guide the eyes.

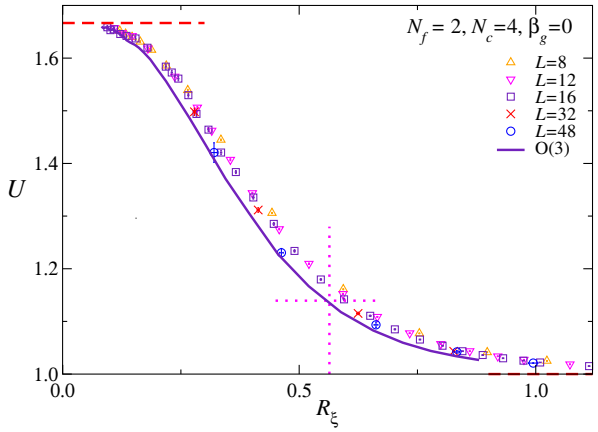

FIG. 13. The Binder parameter U versus R_ξ for $N_f = 2$, $N_c = 4$, and $\beta_g = 0$. The data appear to converge to the O(3) vector universal curve (continuous line). The dotted horizontal and vertical lines correspond to the universal values $U^* = 1.1394(3)$ and $R_\xi^* = 0.5639(2)$ of the O(3) universality class. The dashed horizontal lines correspond to $U = 5/3$ and $U = 1$, the asymptotic values for $R_\xi \to 0$ and $R_\xi \to \infty$.

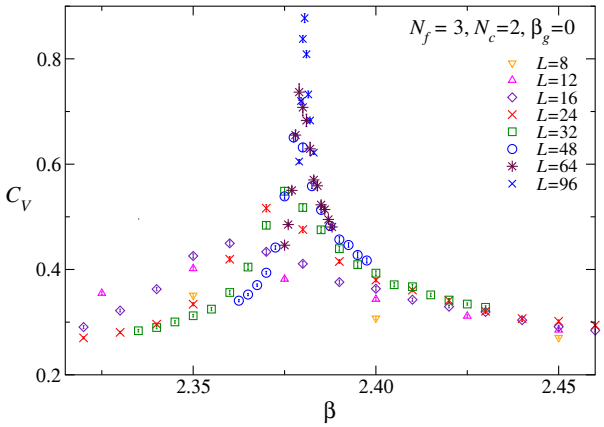

FIG. 14. The specific heat defined in Eq. (30) versus β for $N_c = 2$, $N_f = 3$, and $\beta_g = 0$.

C. FSS analysis for $N_f = 3$

For $N_f = 3$, the LGW effective field theory predicts a first-order phase transition for any number of colors. To verify the prediction, we perform simulations for $N_c = 2$ and $N_c = 3$, always fixing $\beta_g = 0$.

A standard technique to identify first-order phase transitions consists in checking if the maximum value of the susceptibility or of the specific heat scales linearly with the volume. However, for weak first-order transitions such a technique is, in practice, quite often ineffective: the values of L at which such a behavior sets in are far larger than those at which simulations can be performed. This is indeed what happens, as we discuss below, for $N_c = 2$ and 3.

In Fig. 14, we report the specific heat C_V defined in Eq. (30) for $N_c = 2$. It is clear that the specific heat is apparently diverging as L increases. This allows us to conclude that the transition, if continuous, does not belong to a universality class characterized by a negative value of the critical exponent α, like, e.g., the standard O(M) universality classes for any $M \geq 2$ [8].

In the case of weak first-order transitions, a more useful quantity is the Binder parameter U. At a first-order transition, the maximum $U_{\max}$ of U behaves as [58,59]

$$U_{\max} = aV[1 + O(V^{-1})]. \tag{62}$$

On the other hand, at a continuous phase transition, U is bounded as $L \to \infty$. At the critical point, U converges to a universal value U^*, while the data of U corresponding to different values of R_ξ collapse onto a common scaling curve as the volume is increased. Therefore, U has a qualitatively different scaling behavior for first- and second-order transitions. In practice, a first-order transition can be simply identified by verifying that $U_{\max}$ increases with L, without the need of explicitly observing the linear behavior in the volume. A second indication of a first-order transition is provided by the plot of U versus R_ξ. The

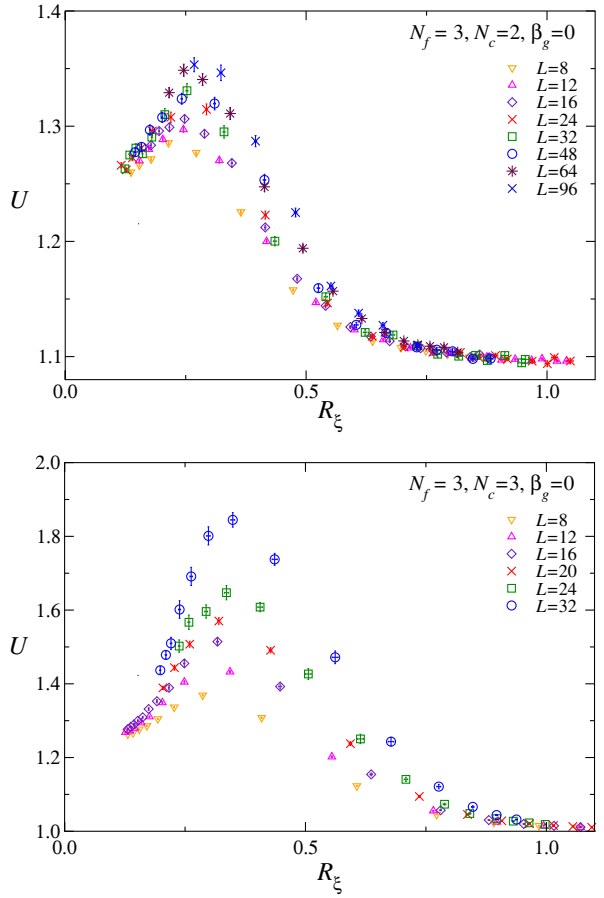

FIG. 15. The Binder parameter U versus R_ξ for $N_f = 3, N_c = 2$ (top) and $N_c = 3$ (bottom), and $\beta_g = 0$. The presence of a maximum of U diverging in the large-L limit is a peculiar feature of the behavior at first-order transitions; see, e.g., Refs. [20,58,59].

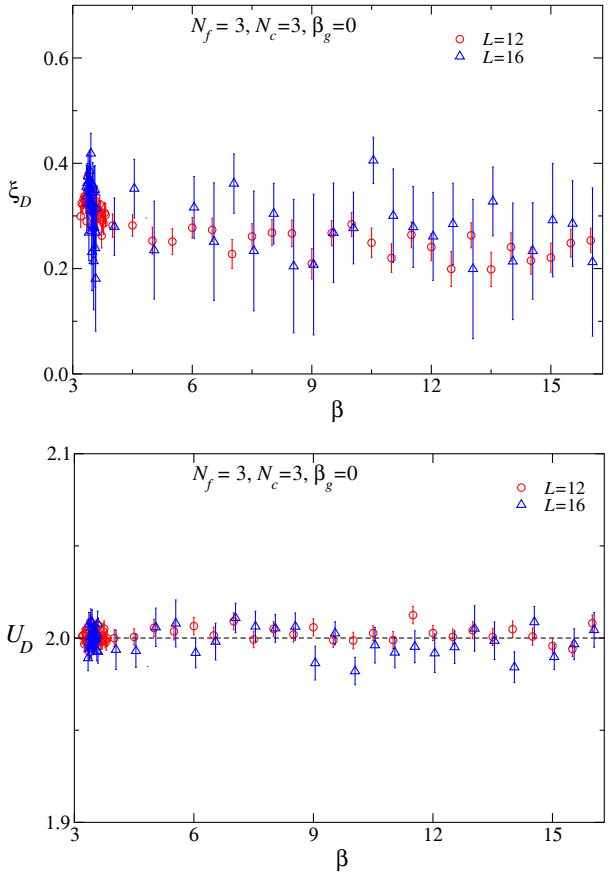

FIG. 16. The correlation length ξ_D (top) and the Binder parameter U_D (bottom) versus β for $N_f = 3$, $N_c = 3$, and $\beta_g = 0$. For this model, the first-order transition occurs at $\beta_c \approx 3.415$.

absence of a data collapse is an early indication of the first-order nature of the transition, as already advocated in Ref. [20]. In Fig. 15, we plot the Binder parameter U versus R_ξ, for $N_c = 2$ and $N_c = 3$, respectively, and $\beta_g = 0$. In neither of the two cases, an acceptable collapse is obtained and the data display a pronounced peak whose height increases with increasing volume. We take the absence of scaling as an evidence that the transition is not continuous, but rather of first order in both cases.

We have also investigated the behavior of the observables related to the breaking of the U(1) flavor symmetry. In Fig. 16, we report the correlation length ξ_D and the Binder parameter U_D, defined in Sec. IV A. Our numerical results show that the correlation length ξ_D is always small, even at the transition point $\beta \approx 3.415$, a clear indication that the U(1) flavor symmetry does not break. The results for the Binder parameter are completely consistent: U_D is always compatible with the high-temperature value $U_D = 2$.

VI. CONCLUSIONS

In this work, we have studied the finite-temperature critical behavior of the lattice multiflavor chromodynamics model defined by the action, Eq. (6). This model is characterized by the presence of a $\mathrm{SU}(N_c)$ gauge symmetry and of a $U(N_f)$ or $\mathrm{Sp}(N_f)$ global symmetry, depending whether $N_c \geq 3$ or $N_c = 2$. In all cases, we find that the system undergoes a finite-temperature phase transition associated with the condensation of a gauge-invariant order parameter: the operator Q_x^{ab} for $N_c \geq 3$ and the operator $\mathcal{T}_x^{\alpha\beta}$ for $N_c = 2$. At the phase transition, the global symmetry $\mathrm{SU}(N_f)$ or $\mathrm{Sp}(N_f)$ is spontaneously broken.

To investigate the possible influence of the gauge d.o.f. on the critical behavior of the model, we determine the universality class of the transition for several values of the number of colors N_c and of the number of flavors N_f, also varying the plaquette-coupling coefficient β_g. In the two-flavor case, we always observe a continuous phase transition, in the 3D O(5) vector universality class for $N_c = 2$ and in the 3D O(3) vector universality class for $N_c = 3, 4$. Instead, for $N_f = 3$, we find results compatible with the presence of a first-order phase transition both for $N_c = 2$ and 3.

These results agree with the predictions of a LGW analysis based on a gauge-invariant order parameter [36], summarized in Table I. Therefore, they indicate the irrelevance of the non-Abelian gauge d.o.f. at the finite-temperature transition. In other words, gauge invariance does not play any role at the transition, apart from that of restricting the fields to the coset $S^M/\mathrm{SU}(N_c)$ where $S^M = \mathrm{SO}(M)/\mathrm{SO}(M-1)$ is the M-dimensional sphere and $M = 2N_cN_f$. Such a conclusion is also consistent with the observed behavior of the correlation function G_V, defined in Eq. (40), which directly involves the gauge d.o.f. In all cases, this correlation function is short ranged at the transition.

These results strongly support the procedure initially advocated by Pisarski and Wilczek in Ref. [12] to study the chiral phase transition in massless QCD, which makes use of gauge-invariant order parameters to analyze the critical behavior of gauge theories when a global symmetry gets spontaneously broken.

We finally note that there are still several points which deserve to be further investigated. For example, in this work, we concentrated on the gauge theory that is obtained by starting from a maximally symmetric $\mathrm{O}(M)$-invariant model and by fixing $\mathrm{Tr} Z_x^\dagger Z_x = 1$. It would be interesting to investigate what happens if one or both of these conditions are relaxed. It would also be interesting to study theories with different global and local symmetries that are different from the ones considered in this work.

ACKNOWLEDGMENTS

Numerical simulations have been performed on the CSN4 cluster of the Scientific Computing Center at INFN-PISA. We thank Daniele Teresi and Omar Zanusso for useful discussions.

APPENDIX A: SYMPLECTIC OBSERVABLES FOR $N_c = 2$

For $N_c = 2$, the order parameter is the symplectic analogue of Q_x defined in Eq. (28). It is a $2N_f \times 2N_f$ Hermitian traceless matrix, which satisfies the relation

$$J\bar{\mathcal{T}}J + \mathcal{T} = 0, \tag{A1}$$

which follows from Eq. (16). It is thus an element of the $\mathfrak{sp}(N_f)$ algebra [41]. It can be parametrized in the block form

$$\mathcal{T} = \begin{pmatrix} A_1 & A_2 \\ A_3 & A_4 \end{pmatrix}, \tag{A2}$$

where A_1, A_2, A_3, and A_4 are $N_f \times N_f$ matrices, A_1 is Hermitian and traceless, A_3 is antisymmetric and

$$A_4 = \bar{A}_1, \qquad A_3 = -\bar{A}_2. \tag{A3}$$

It is not difficult to show that $\mathcal{T}$ can be expressed in terms of the two order parameters Q_x^{fg} and D_x^{fg}. Indeed, we have

$$A_1 = Q, \qquad A_3 = -D. \tag{A4}$$

This result implies that the critical behavior encoded in $\mathcal{T}_x^{\alpha\beta}$ can be also investigated by studying Q_x^{fg}. However, some care should be exercised, when comparing the results with the $\mathrm{Sp}(N_f)$ predictions. We define the correlation function of the $\mathcal{T}$ field,:

$$G_\Gamma(\boldsymbol{x}-\boldsymbol{y}) = \langle \mathrm{Tr}\mathcal{T}_{\boldsymbol{x}}\mathcal{T}_{\boldsymbol{y}}\rangle. \tag{A5}$$

Such a correlation can be related to the correlation of the Q field defined in Eq. (32). We use the relation

$$\langle \mathcal{T}_x^{\alpha\beta}\mathcal{T}_y^{\gamma\delta}\rangle = \frac{1}{2(N_f-1)(2N_f+1)} G_\Gamma(\boldsymbol{x}-\boldsymbol{y}) \times \left(J^{\alpha\gamma}J^{\beta\delta} + \delta^{\alpha\delta}\delta^{\beta\gamma} - \frac{1}{N_f}\delta^{\alpha\beta}\delta^{\gamma\delta}\right), \tag{A6}$$

which follows from the $\mathrm{Sp}(N_f)$ invariance of the theory. We obtain the relation

$$G_\Gamma(\boldsymbol{x}) = \frac{2(2N_f+1)}{(N_f+1)} G(\boldsymbol{x}). \tag{A7}$$

It implies that, if one uses Eq. (34), the same correlation length is obtained from $G_\Gamma(\boldsymbol{x})$ or $G(\boldsymbol{x})$. The behavior of the Binder parameter is more involved. For $N_c = 2$, the natural Binder parameter is

$$U_\Gamma = \frac{\langle \nu_2^2\rangle}{\langle \nu_2\rangle^2}, \qquad \nu_2 = \frac{1}{V^2}\sum_{\boldsymbol{xy}} \mathrm{Tr}\mathcal{T}_{\boldsymbol{x}}\mathcal{T}_{\boldsymbol{y}}. \tag{A8}$$

In general, such a quantity is not related to U defined in Eq. (35), except for $N_f = 2$, as we discuss below.

For $N_f = 2$, the global invariance group is isomorphic to SO(5). It is useful to make this correspondence explicit. We can rewrite the blocks A_1 and A_3 in Eq. (A2) as

$$A_1 = \begin{pmatrix} \phi_3 & \phi_1 - i\phi_2 \\ \phi_1 + i\phi_2 & -\phi_3 \end{pmatrix}, \qquad A_3 = \begin{pmatrix} 0 & \phi_4 + i\phi_5 \\ -\phi_4 - i\phi_5 & 0 \end{pmatrix}. \tag{A9}$$

Since

$$(\mathcal{T}^2)^{\alpha\beta} = \frac{1}{4}\delta^{\alpha\beta}, \tag{A10}$$

we can verify that

$$\sum_{i=1}^{5} \phi_i^2 = \frac{1}{4}. \tag{A11}$$

Moreover, one can easily verify that, under infinitesimal Sp(2) transformations, the vector $(\phi_1, \ldots, \phi_5)$ transforms as an SO(5) vector. Thus, the redefinition $\mathcal{T} \to \phi$ explicitly realizes the isomorphism between $\mathrm{Sp}(2)/\mathbb{Z}_2$ and SO(5). Since

$$\mathrm{Tr}Q_{\boldsymbol{x}}Q_{\boldsymbol{y}} = 2\sum_{a=1}^{3} \phi_{\boldsymbol{x}}^a\phi_{\boldsymbol{y}}^a, \qquad \bar{D}_{\boldsymbol{x}}D_{\boldsymbol{y}} = \sum_{a=4}^{5} \phi_{\boldsymbol{x}}^a\phi_{\boldsymbol{y}}^a, \tag{A12}$$

we obtain the relations

$$G_\Gamma(\boldsymbol{x}-\boldsymbol{y}) = 4\langle \boldsymbol{\phi}_{\boldsymbol{x}}\cdot\boldsymbol{\phi}_{\boldsymbol{y}}\rangle, \qquad G(\boldsymbol{x}-\boldsymbol{y}) = \frac{3}{20}G_\Gamma(\boldsymbol{x}-\boldsymbol{y}), \qquad G_D(\boldsymbol{x}-\boldsymbol{y}) = \frac{1}{10}G_\Gamma(\boldsymbol{x}-\boldsymbol{y}), \tag{A13}$$

where we have used the O(5) symmetry of the theory. For the Binder parameters, we have

$$U_\Gamma = \frac{\langle \nu_{2\phi}^2\rangle}{\langle \nu_{2\phi}\rangle^2}, \qquad \nu_{2\phi} = \frac{1}{V^2}\sum_{\boldsymbol{xy}} \langle \boldsymbol{\phi}_{\boldsymbol{x}}\cdot\boldsymbol{\phi}_{\boldsymbol{y}}\rangle, \tag{A14}$$

which shows that U_Γ corresponds to the usual O(5) Binder parameter, and

$$U = \frac{25}{21}U_\Gamma, \qquad U_D = \frac{10}{7}U_\Gamma. \tag{A15}$$

APPENDIX B: SYMPLECTIC LANDAU-GINZBURG-WILSON THEORY FOR $N_c = 2$

To define the LGW theory for $N_c = 2$, we introduce a coarse-grained continuum analog Ψ of $\mathcal{T}$, which satisfies the condition

$$J\bar{\Psi}J + \Psi = 0. \tag{B1}$$

The corresponding action is given in Eq. (22). For $N_f = 2$, we obtain the O(5) LGW model. Indeed, in this case, we can set

$$\Psi = \begin{pmatrix} A_1 & A_2 \\ A_3 & A_4 \end{pmatrix}, \tag{B2}$$

where

$$A_1 = \begin{pmatrix} \psi_3 & \psi_1 - i\psi_2 \\ \psi_1 + i\psi_2 & -\psi_3 \end{pmatrix},$$
$$A_3 = \begin{pmatrix} 0 & \psi_4 + i\psi_5 \\ -\psi_4 - i\psi_5 & 0 \end{pmatrix}, \tag{B3}$$

and $A_4 = \bar{A}_1$, $A_3 = -\bar{A}_2$, from which it easily follows that

$$\Psi^2 = I\left(\sum_{i=1}^{5} \psi^2\right), \qquad \mathrm{Tr}\Psi^3 = 0. \tag{B4}$$

Thus, the LGW effective theory for Ψ in the Sp(2) case is equivalent to that for the O(5) vector model.

APPENDIX C: THE BEHAVIOR FOR $\beta \to \infty$

In this appendix, we study the large-β limit of the model described by the action S_g, Eq. (6), for $\beta_g = 0$. As the system is ferromagnetic, the global minimum of the β-dependent part of the action is obtained by minimizing the contribution of each link. This is obtained by setting

$$Z_{\boldsymbol{x}} = U_{\boldsymbol{x},\mu} Z_{\boldsymbol{x}+\hat{\mu}} \tag{C1}$$

on each link. This relation implies that

$$Q_{\boldsymbol{x}} = Q_{\boldsymbol{x}+\hat{\mu}}, \qquad D_{\boldsymbol{x}} = D_{\boldsymbol{x}+\hat{\mu}} \tag{C2}$$

on each link, where $Q_{\boldsymbol{x}}$ and $D_{\boldsymbol{x}}$ are the order parameters defined in Eqs. (21) and (26). The unit-length condition implies that $Q_{\boldsymbol{x}}$ is nonvanishing: the system is fully ordered in the limit $\beta \to \infty$ and therefore the $\mathrm{SU}(N_f)$ subgroup is broken at zero temperature. As for the U(1) order parameter $D_{\boldsymbol{x}}$, we shall show below that $D_{\boldsymbol{x}}$ is nonvanishing for $N_c = 2$. This is obvious as the U(1) subgroup is a subgroup of the $\mathrm{Sp}(N_f)$ symmetry group, which is broken. On the other hand, for $N_c \geq 3$, we find $D_{\boldsymbol{x}} = 0$: the U(1) flavor symmetry is not broken.

Let us now consider any closed path $C_{\boldsymbol{x}}$ that starts and ends in the same point $\boldsymbol{x}$. By repeated applications of condition (C1), we obtain the consistency condition

$$Z_{\boldsymbol{x}}^{af} = \sum_b \left[\prod_{l\in C_{\boldsymbol{x}}} U_l\right]^{ab} Z_{\boldsymbol{x}}^{bf}. \tag{C3}$$

This relation implies that the product of the links along the path has at least one unit eigenvalue. For an SU(2) matrix, this implies that the product is the identity matrix. Therefore, for $N_c = 2$, we can set $U_{\boldsymbol{x},\hat{\mu}} = 1$ modulo gauge transformations. For $N_c \geq 3$, we obtain the condition

$$\prod_{l\in C_{\boldsymbol{x}}} U_l = V_{\boldsymbol{x}}^{\dagger} W V_{\boldsymbol{x}}, \tag{C4}$$

with $V_{\boldsymbol{x}} \in SU(N_c)$ and

$$W = \begin{pmatrix} \hat{W} & 0 \\ 0 & 1 \end{pmatrix}, \tag{C5}$$

where $\hat{W}$ is an $\mathrm{SU}(N_c - 1)$ matrix. If $\hat{W}$ does not have unit eigenvalues (this is the case for a generic unitary matrix), then

$$Z_{\boldsymbol{x}} = V_{\boldsymbol{x}}^{\dagger} A, \qquad A = \begin{pmatrix} 0 \\ \hat{z} \end{pmatrix}, \tag{C6}$$

where A is an $N_c \times N_f$ matrix such that $A_{ij} = 0$ for any $i = 1, \ldots N_c - 1$; $\hat{z}$ is a unit vector of N_f elements.

To obtain more information on the gauge configurations relevant for $\beta \to \infty$, we performed simulations for $\beta_g = 0$ on small lattices (2^3 and 4^3) for very large β values (from $\beta = 50$ up to $\beta = 300$) and then we extrapolated the results to $\beta \to \infty$. Results for different quantities are reported in Tables IV and V. Note that we are indeed probing the system in the large β regime as the average energy E defined in Eq. (30) converges to -3. In Tables IV and V, we also report the average gauge energy defined in Eq. (31). For $N_c = 2$, results are consistent with the plaquette being the identity matrix. For $N_c \geq 3$, data for the average gauge energy, cf. Eq. (31), are consistent with

$$E_g = \frac{1}{N_c}. \tag{C7}$$

Note that this is not an exact equality for finite L. However, deviations decrease as L increases from two to four. Such a result can be explained by assuming that the relevant configurations are such that all plaquettes can be rewritten in the form (C4), where W is given in Eq. (C5). Indeed, if this is the case and $\hat{W}$ is randomly distributed, we obtain the result (C7). Of course, we are not claiming that all minimizing configurations are such that Eqs. (C5)

TABLE IV. Asymptotic values for $\beta \to \infty$ on a 2^3 lattice at $\beta_g = 0$.

(N_c, N_f)	E_g	$E/3$	U	Eq. (C11)	$\mathrm{Tr}P^2$	Eq. (C10)
(2, 2)	0.99998(2)	−0.999992(6)	1.191(2)	1.19048…	0.800(1)	0.8
(2, 3)	1.00000(1)	−1.000010(5)	1.0940(5)	1.09375…	0.714(2)	0.714286…
(2, 4)	1.00001(1)	−1.000000(4)	1.0582(3)	1.05818…	0.666(1)	0.666667…
(2, 5)	1.00000(1)	−1.000000(6)	1.0400(3)	1.04006…	0.636(1)	0.636364…
(2, 6)	0.999990(6)	−1.000000(4)	1.0294(2)	1.02939…	0.615(2)	0.615385…
(3, 2)	0.3347(3)	−1.000005(6)	1.0000000(1)		1.00001(1)	
(3, 3)	0.3369(4)	−0.999993(6)	1.0000000(6)		0.99999(1)	
(3, 4)	0.3382(4)	−1.000000(7)	1.0000000(6)		1.00000(1)	
(3, 5)	0.3413(4)	−1.000000(5)	1.0000000(1)		1.00000(1)	
(3, 6)	0.3463(4)	−1.000000(5)	1.00000000(4)		0.99999(1)	
(4, 2)	0.2500(2)	−0.99999(1)	1.0000000(4)		1.00000(1)	
(4, 3)	0.2510(2)	−1.00001(1)	1.0000000(2)		1.00001(2)	
(4, 4)	0.2513(3)	−0.99995(4)	1.0000000(3)		0.99992(8)	
(4, 5)	0.2520(4)	−1.000010(7)	1.0000000(1)		1.00002(2)	
(4, 6)	0.2527(3)	−1.000000(6)	1.0000000(1)		0.99999(1)	

TABLE V. Asymptotic values for $\beta \to \infty$ on a 4^3 lattice at $\beta_g = 0$.

(N_c, N_f)	E_g	$E/3$	U	Eq. (C11)	$\mathrm{Tr}P^2$	Eq. (C10)
(2, 2)	0.99998(2)	−0.999999(2)	1.195(3)	1.19048…	0.798(1)	0.8
(2, 3)	1.000000(6)	−1.000000(2)	1.094(1)	1.09375…	0.714(3)	0.714286…
(2, 4)	0.999999(3)	−1.000000(3)	1.0580(5)	1.05818…	0.666(2)	0.666667…
(2, 5)	1.000000(3)	−1.000000(3)	1.040(1)	1.04006…	0.637(2)	0.636364…
(2, 6)	1.000000(3)	−0.999988(5)	1.0293(5)	1.02939…	0.615(2)	0.615385…
(3, 2)	0.3344(2)	−1.000000(3)	1.000000(3)		1.000000(6)	
(3, 3)	0.3356(2)	−1.000000(3)	1.000000(3)		0.999999(6)	
(3, 4)	0.3368(2)	−0.999999(3)	1.000000(3)		1.000008(8)	
(3, 5)	0.3375(2)	−1.000000(3)	1.00000000(5)		1.00001(1)	
(3, 6)	0.3385(2)	−0.999996(4)	1.00000000(2)		0.99999(1)	
(4, 2)	0.2501(2)	−1.00000(1)	1.0000000(1)		0.99999(2)	

and (C6) hold. We only claim that the number of these configurations is exponentially larger in the lattice volume than the others, so that they dominate the effective asymptotic behavior. As a check, we have determined the average of P^2, where $P_{\boldsymbol{x}}^{fg}$ is defined by

$$P_{\boldsymbol{x}}^{fg} = \sum_a \bar{Z}_{\boldsymbol{x}}^{af} Z_{\boldsymbol{x}}^{ag}. \tag{C8}$$

In general, such an operator is not a projector, i.e., $P^2 \neq P$. However, if the Z fields satisfy Eq. (C6), we have $P^2 = P$ and in particular $\mathrm{Tr}P^2 = 1$. The results reported in Tables IV and V are in perfect agreement with this result, confirming the above analysis.

If the relevant configurations have the form (C6) it is immediate to prove that $D_{\boldsymbol{x}} = 0$ everywhere. The U(1) flavor symmetry is not broken at $\beta = \infty$, at least for $\beta_g = 0$. It is easy to understand under which conditions the order parameter $D_{\boldsymbol{x}}$ is not zero. If we imagine the field Z^{af} as a collection of N_f complex vectors of dimension N_c, then $D_{\boldsymbol{x}}$ does not vanish if N_c of these vectors are nonvanishing and linearly independent. If this occurs, the consistency condition (C3) implies that the product of the links along any path has N_c unit eigenvalues. As the product is an $\mathrm{SU}(N_c)$ matrix, it must be equal to the identity matrix, which implies that all gauge fields are equivalent to the identity modulo gauge transformations. This argument shows therefore that the U(1) symmetry can be broken only if the relevant configurations are characterized by the triviality of the gauge fields. For $N_c \geq 3$ and $\beta_g = 0$, this does not occur and the U(1) symmetry is unbroken. For $\beta_g = \infty$, there is no gauge dependence and the U(1) symmetry is broken, an obvious result given that the U(1) group is a subgroup of the larger $O(2N_fN_c)$ group. As we expect the gauge energy E_g to depend smoothly on β_g, we should always have $E_g < 1$ for finite β_g: there are relevant nontrivial gauge configurations that always forbid the breaking of the U(1) symmetry.

Let us finally discuss the behavior for $N_c = 2$. In this case, we can set $U_{\boldsymbol{x},\hat{\mu}} = 1$ everywhere. Equation (C1)

implies that $Z_{\boldsymbol{x}}^{af}$ takes the same value on each link. Thus, the average of any quantity $\mathcal{O}(Z_{\boldsymbol{x}})$ can be obtained as

$$\langle \mathcal{O}((Z_{\boldsymbol{x}}))\rangle = \int [dA]\mathcal{O}(A), \tag{C9}$$

where A is an $N_c \times N_f$ matrix ($N_c = 2$) and $[dA]$ is the normalized invariant integration measure over the $N_c N_f$-dimensional complex sphere defined by $\mathrm{Tr}A^\dagger A = 1$.

We obtain

$$\langle \mathrm{Tr}P_{\boldsymbol{x}}^2\rangle = \int [dA]\mathrm{Tr}[(A^\dagger A)^2] = \frac{N_f + N_c}{1 + N_f N_c} \tag{C10}$$

and

$$U = \frac{(1 + N_f N_c)(N_f N_c + 4N_f^2 + N_f^3 N_c - 6)}{(N_f^2 - 1)(2 + N_f N_c)(3 + N_f N_c)}, \tag{C11}$$

which again are consistent with the numerical data in Tables IV and V for $N_c = 2$. Note that the results for U are consistent with $U_\Gamma = 1$ when $N_f = 2$; see Eq. (A15).

The results that we have obtained for $N_c = 2$ do not depend on the dimensionality of the system. On the other hand, for $N_c \geq 3$, the conclusions we have obtained rely on the fact that the relevant configurations have the form (C5) and (C6), a claim that is only justified by the numerical study we have performed on cubic lattices. We expect, but we do not have a proof, that the same result holds in any dimension.

[1] P. W. Anderson, *Basic Notions of Condensed Matter Physics* (The Benjamin/Cummings Publishing Company, Menlo Park, California, 1984).
[2] S. Weinberg, *The Quantum Theory of Fields* (Cambridge University Press, Cambridge, United Kingdom, 2005).
[3] P. W. Anderson, Plasmons, gauge invariance, and mass, Phys. Rev. **130**, 439 (1963); Superconductivity: Higgs, Anderson and all that, Nat. Phys. **11**, 93 (2015).
[4] S. Sachdev, Topological order, emergent gauge fields, and Fermi surface reconstruction, Rep. Prog. Phys. **82**, 014001 (2019).
[5] L. D. Landau and E. M. Lifshitz, *Statistical Physics. Part I*, 3rd ed. (Elsevier Butterworth-Heinemann, Oxford, 1980).
[6] K. G. Wilson and J. Kogut, The renormalization group and the ϵ expansion, Phys. Rep. **12**, 75 (1974).
[7] M. E. Fisher, The renormalization group in the theory of critical behavior, Rev. Mod. Phys. **47**, 543 (1975).
[8] A. Pelissetto and E. Vicari, Critical phenomena and renormalization group theory, Phys. Rep. **368**, 549 (2002).
[9] J. Zinn Justin, *Quantum Field Theory and Critical Phenomena* (Oxford University Press, Oxford, 2002).
[10] T. Senthil, L. Balents, S. Sachdev, A. Vishwanath, and M. P. A. Fisher, Quantum criticality beyond the Landau-Ginzburg-Wilson paradigm, Phys. Rev. B **70**, 144407 (2004).
[11] C. Wang, A. Nahum, M. A. Metlitski, C. Xu, and T. Senthil, Deconfined Quantum Critical Points: Symmetries and Dualities, Phys. Rev. X **7**, 031051 (2017).
[12] R. D. Pisarski and F. Wilczek, Remarks on the chiral phase transition in chromodynamics, Phys. Rev. D **29**, 338 (1984).
[13] A. Butti, A. Pelissetto, and E. Vicari, On the nature of the finite-temperature transition in QCD, J. High Energy Phys. 08 (2003) 029.
[14] A. Pelissetto and E. Vicari, Relevance of the axial anomaly at the finite-temperature chiral transition in QCD, Phys. Rev. D **88**, 105018 (2013).
[15] M. D'Elia, High-Temperature QCD: Theory overview, Nucl. Phys. **A982**, 99 (2019).
[16] S. Sharma, Recent Progress on the QCD Phase Diagram, Proc. Sci., LATTICE2018 (**2019**) 009.
[17] Y.-Z. You, Y.-C. He, C. Xu, and A. Vishwanath, Symmetric Fermion Mass Generation as Deconfined Quantum Criticality, Phys. Rev. X **8**, 011026 (2018).
[18] Y.-Z. You, Y.-C. He, A. Vishwanath, and C. Xu, From bosonic topological transition to symmetric fermion mass generation, Phys. Rev. B **97**, 125112 (2018).
[19] A. Thomson and S. Sachdev, Fermionic Spinon Theory of Square Lattice Spin Liquids near the Néel State, Phys. Rev. X **8**, 011012 (2018).
[20] A. Pelissetto and E. Vicari, Three-dimensional ferromagnetic CP^{N-1} models, Phys. Rev. E **100**, 022122 (2019).
[21] A. Pelissetto and E. Vicari, Multicomponent compact Abelian-Higgs lattice models, Phys. Rev. E **100**, 042134 (2019).
[22] A. Nahum, J. T. Chalker, P. Serna, M. Ortuño, and A. M. Somoza, 3D Loop Models and the CP^{n-1} Sigma Model, Phys. Rev. Lett. **107**, 110601 (2011).
[23] A. Nahum, J. T. Chalker, P. Serna, M. Ortuño, and A. M. Somoza, Phase transitions in three-dimensional loop models and the CP^{n-1} sigma model, Phys. Rev. B **88**, 134411 (2013).
[24] A. Pelissetto, A. Tripodo, and E. Vicari, Landau-Ginzburg-Wilson approach to critical phenomena in the presence of gauge symmetries, Phys. Rev. D **96**, 034505 (2017).
[25] A. Pelissetto, A. Tripodo, and E. Vicari, Criticality of O(N) symmetric models in the presence of discrete gauge symmetries, Phys. Rev. E **97**, 012123 (2018).
[26] S. Gazit, F. F. Assaad, S. Sachdev, A. Vishwanath, and C. Wang, Confinement transition of Z_2 gauge theories coupled to massless fermions: Emergent QCD_3 and SO(5) symmetry, Proc. Natl. Acad. Sci. U.S.A. **115**, E6987 (2018).
[27] S. Sachdev, H. D. Scammell, M. S. Scheurer, and G. Tarnopolsky, Gauge theory for the cuprates near optimal doping, Phys. Rev. B **99**, 054516 (2019).

[28] S. Nadkarni, The SU(2) adjoint Higgs model in three dimensions, Nucl. Phys. **B334**, 559 (1990).
[29] K. Kajantie, K. Rummukainen, and M. E. Shaposhnikov, A Lattice Monte Carlo study of the hot electroweak phase transition, Nucl. Phys. **B407**, 356 (1993).
[30] W. Buchmüller and O. Philipsen, Phase structure and phase transition of the SU(2) Higgs model in three-dimensions, Nucl. Phys. **B443**, 47 (1995).
[31] K. Kajantie, M. Laine, K. Rummukainen, and M. E. Shaposhnikov, Is There a Hot Electroweak Phase Transition at $m_H \gtrsim m_W$?, Phys. Rev. Lett. **77**, 2887 (1996).
[32] A. Hart, O. Philipsen, J. D. Stack, and M. Teper, On the phase diagram of the SU(2) adjoint Higgs model in $(2+1)$-dimensions, Phys. Lett. B **396**, 217 (1997).
[33] K. Osterwalder and E. Seiler, Gauge field theories on the lattice, Ann. Phys. (NY) **110**, 440 (1978).
[34] E. Fradkin and S. Shenker, Phase diagrams of lattice gauge theories with Higgs fields, Phys. Rev. D **19**, 3682 (1979).
[35] S. Dimopoulos, S. Raby, and L. Susskind, Light composite fermions, Nucl. Phys. **B173**, 208 (1980).
[36] C. Bonati, A. Pelissetto, and E. Vicari, Phase Diagram, Symmetry Breaking, and Critical Behavior of Three-Dimensional Lattice Multiflavor Scalar Chromodynamics, Phys. Rev. Lett. **123**, 232002 (2019).
[37] K. G. Wilson, Confinement of quarks, Phys. Rev. D **10**, 2445 (1974).
[38] H. Georgi, *Weak Interactions and Modern Particle Theory* (The Benjamin/Cummings Publishing Company, Menlo Park, California, 1984).
[39] P. Arnold and L. G. Yaffe, The ϵ expansion and the electroweak phase transition, Phys. Rev. D **49**, 3003 (1994).
[40] P. S. Bhupal Dev and A. Pilaftsis, Maximally symmetric two Higgs doublet model with natural standard model alignment, J. High Energy Phys. 12 (2014) 024; Erratum, J. High Energy Phys. 11 (2015) 147.
[41] B. Simon, *Representations of Finite and Compact Groups* (American Mathematical Society, Providence, 1996).
[42] A. Das, Phase transition in $\mathrm{SU}(N) \times \mathrm{U}(1)$ gauge theory with many fundamental bosons, Phys. Rev. B **97**, 214429 (2018).
[43] V. Alba, A. Pelissetto, and E. Vicari, The uniformly frustrated two-dimensional XY model in the limit of weak frustration, J. Phys. A **41**, 175001 (2008).
[44] M. Creutz, Monte Carlo study of quantized SU(2) gauge theory, Phys. Rev. D **21**, 2308 (1980).
[45] A. D. Kennedy and B. J. Pendleton, Improved heat bath method for Monte Carlo calculations in lattice gauge theories, Phys. Lett. **156B**, 393 (1985).
[46] M. Creutz, Overrelaxation and Monte Carlo simulation, Phys. Rev. D **36**, 515 (1987).
[47] N. Cabibbo and E. Marinari, A new method for updating SU(N) matrices in computer simulations of gauge theories, Phys. Lett. **119B**, 387 (1982).
[48] N. Metropolis, A. W. Rosenbluth, M. N. Rosenbluth, A. H. Teller, and E. Teller, Equation of state calculations by fast computing machines, J. Chem. Phys. **21**, 1087 (1953).
[49] S. A. Antonenko and A. I. Sokolov, Critical exponents for a three-dimensional $\mathrm{O}(n)$-symmetric model with $n > 3$, Phys. Rev. E **51**, 1894 (1995).
[50] M. Hasenbusch, A. Pelissetto, and E. Vicari, Instability of the O(5) critical behavior in the SO(5) theory of high-T_c superconductors, Phys. Rev. B **72**, 014532 (2005).
[51] L. A. Fernández, V. Martín-Mayor, D. Sciretti, A. Tarancón, and J. L. Velasco, Numerical study of the enlarged O(5) symmetry of the 3-D antiferromagnetic RP^2 spin model, Phys. Lett. B **628**, 281 (2005).
[52] P. Calabrese, A. Pelissetto, and E. Vicari, Multicritical behavior of $\mathrm{O}(n_1) \oplus \mathrm{O}(n_2)$-symmetric systems, Phys. Rev. B **67**, 054505 (2003).
[53] F. Delfino, A. Pelissetto, and E. Vicari, Three-dimensional antiferromagnetic CP^{N-1} models, Phys. Rev. E **91**, 052109 (2015).
[54] M. Hasenbusch and E. Vicari, Anisotropic perturbations in 3D $\mathrm{O}(N)$ vector models, Phys. Rev. B **84**, 125136 (2011).
[55] M. Campostrini, M. Hasenbusch, A. Pelissetto, P. Rossi, and E. Vicari, Critical exponents and equation of state of the three-dimensional Heisenberg universality class, Phys. Rev. B **65**, 144520 (2002).
[56] R. Guida and J. Zinn-Justin, Critical exponents of N-vector models, J. Phys. A **31**, 8103 (1998).
[57] M. Campostrini, A. Pelissetto, P. Rossi, and E. Vicari, Four-point renormalized coupling in $\mathrm{O}(N)$ models, Nucl. Phys. **B459**, 207 (1996).
[58] M. S. S. Challa, D. P. Landau, and K. Binder, Finite-size effects at temperature-driven first-order transitions, Phys. Rev. B **34**, 1841 (1986).
[59] K. Vollmayr, J. D. Reger, M. Scheucher, and K. Binder, Finite size effects at thermally-driven first order phase transitions: A phenomenological theory of the order parameter distribution, Z. Phys. B **91**, 113 (1993).